Rheological structure and deformation of subducted slabs in the mantle transition zone: implications for mantle circulation and deep earthquakes

Shun-ichiro Karato [a,*], Michael R. Riedel [b], David A. Yuen [a,c]

[a] *Department of Geology and Geophysics, University of Minnesota, Minneapolis, MN 55455, USA*
[b] *GeoForschungs Zentrum, Telegrafenberg, Potsdam D-14473, Germany*
[c] *Minnesota Supercomputer Institute, University of Minnesota, Minneapolis, MN 55415-1227, USA*

Abstract

Rheological structure of subducted slabs of oceanic lithosphere in the mantle transition zone is investigated based on mineral physics observations incorporating grain-size, stress, temperature and pressure dependence of rheology. It is shown that the rheological structure of slabs depends strongly on subduction parameters through temperature that controls the grain-size of spinel (ringwoodite) and the magnitude of forces acting on a slab. We use a theoretical model of grain-size evolution associated with the olivine–spinel transformation, plastic flow laws of olivine and spinel combined with a thermal model of subducting slab in which the effect of latent heat release is incorporated. Three deformation mechanisms for olivine and spinel (diffusional creep, power-law (dislocation) creep and the Peierls mechanism) are considered. Due to the large variation in temperature, stress and grain-size, a subducting slab is shown to have a complicated rheological structure which varies both laterally and with depth. A cold slab in the deep transition zone is characterized by a weak, fine-grained spinel region surrounded by narrow but strong regions. The flexural rigidity and the curvature of a slab are calculated using a new formulation in which the effects of stress-dependent rheology is incorporated in a self-consistent fashion. Although uncertainties in both the transformation kinetics and the rheology of high pressure phases are still large, the general trend of dependence of slab flexural rigidity and the curvature on the subduction parameters is well constrained. Slabs with very low thermal parameters (warm slabs) are weak, but slabs with large thermal parameters (cold slabs) are also weak due to small spinel grain-size and large external force (bending moment). Slabs with intermediate thermal parameters will have a relatively large flexural rigidity and could penetrate into the lower mantle without much deformation. Thus the 660 km discontinuity may work as a rheological filter for mantle convection. This prediction provides a natural explanation for a paradoxical observation that significant deformation of slabs is observed exclusively in the western Pacific where temperatures of the slabs are considered to be low.

Our slab rheology models also have important implications for deep earthquakes. Overall rheological weakening of slabs in the deep transition zone results in high rates of deformation under relatively low temperatures providing a favorable environment for thermal runaway instability (adiabatic shear instability). Our model predicts heterogeneous energy dissipation as a result of heterogeneous rheology: energy dissipation in deep, cold slabs is concentrated in high strength regions surrounding a weak, fine-grained spinel core. The regions of high energy dissipation are prone to thermal runaway instability and are likely

* Corresponding author. Present address: Department of Geology and Geophysics, Yale University, New Haven, CT 06520-8109;
Tel.: +1-203-432-3164; fax: +1-203-432-3134.
E-mail address: karato@yale.edu (S. Karato).

to be seismogenic. The width of this seismogenic region is well constrained by our model and is predicted to be ∼40–60 km which is in excellent agreement with seismological observations. Other features of deep earthquakes including low seismic efficiency and low aftershock activities can also be explained by the thermal instability model. © 2001 Elsevier Science B.V. All rights reserved.

1. Introduction

Deformation of subducted slabs consumes a large amount of energy and therefore subduction is considered to be the most important and violent of the processes that control the dynamics of the solid Earth (e.g. Forsyth and Uyeda, 1975; Chapple and Tullis, 1977). Presently, a number of problems related to subduction remain unsolved particularly those concerning deep processes. They include the cause of regional variation in the nature of interaction between slabs and the transition zone that has an important influence on the style of mantle convection and the origin of deep earthquakes. A better understanding of these problems requires the detailed understanding of rheological properties of minerals under deep mantle conditions. However, in most previous models of slab deformation, highly simplified rheological properties such as homogenous rheology across a slab and/or Newtonian rheology sometimes with a weak temperature dependence were assumed (Zhong and Gurnis, 1995; Christensen, 1996; Houseman and Gubbins, 1997; Schmeling et al., 1999).

Complications of mantle convection caused by the slab-transition zone interactions have been emphasized by numerical modeling studies that demonstrated the important effects of the 660 km discontinuity on the style of mantle convection (Christensen and Yuen, 1984; Honda et al., 1993; Tackley et al., 1993; Davies, 1995). These studies also showed that the nature of slab-transition zone interaction is highly sensitive to subtle differences in material properties and/or the Rayleigh number (Christensen and Yuen, 1984, 1985; King and Ita, 1995; Davies, 1995), and therefore one might expect a variety of slab-transition zone interactions in the present Earth. In fact, in some portions of the western Pacific, slabs appear to be deflected horizontally above the 660 km discontinuity and there is no clear image of slabs in most of the lower mantle (van der Hilst et al., 1991;

Fukao et al., 1992; Ding and Grand, 1994; Bijwaard et al., 1998). In contrast, in most of the eastern Pacific (and in the Tethys), slabs appear to penetrate into the lower mantle without much deformation (Grand, 1994; van der Hilst et al., 1997). This is a rather paradoxical observation, because slabs in the eastern Pacific are expected to be warm and hence should deform more easily than the relatively cold ones in the western Pacific.

Another puzzling observation is the occurrence of deep earthquakes which occur under temperature–pressure conditions where brittle failure is unlikely to occur. Various models of deep earthquakes have been proposed including a thermal runaway instability (adiabatic instability) model (Griggs and Baker, 1969; Ogawa, 1987; Hobbs and Ord, 1988), a transformational faulting model (Kirby, 1987; Green and Burnley, 1989; Kirby et al., 1991, 1996; Green, 1994; Green and Houston, 1995) and instability caused by amorphization of hydrous minerals (Meade and Jeanloz, 1991). However, none of the existing models provide satisfactory explanations for important seismological observations such as the geometry of faults, seismic efficiency and the frequency of aftershocks. Thus, the paradox of deep earthquakes has not been solved despite the recent claim by Green (1994).

The main purpose of this study is to provide a better rheological model of deep slabs in the transition zone to answer the above questions using mineral physics data in comparison to geodynamic observations. A simpler model has been published (Riedel and Karato, 1997) in which only the role of grain-size reduction was considered. However, this earlier treatment contained several limitations including the formulation of slab deformation assuming a constant strain-rate and the large uncertainties in rheological parameters available at that time. In addition, comparisons with geodynamic observations were not made in detail. In this paper, we have extended this earlier work by

including the use of a new self-consistent formulation of slab deformation and the use of new better-constrained rheological data that have recently become available. We first summarize geophysical observations on slab deformation and seek some correlation between slab deformation and slab thermal parameters. We then present a new method of calculating the "flexural rigidity" of a slab in a self-consistent fashion. We consider both the effects of phase transformations to modify the grain-size of newly formed spinel and of the stress-dependent deformation mechanisms in silicates. We then compare the calculated variation of flexural rigidity with subduction parameters and geodynamic observations related to slab deformation. Some implications of the present model for deep earthquakes will also be discussed including the geometry of faults, seismic efficiency and the frequency of aftershocks.

2. Geophysical observations of slab deformation

We use the geometry of Wadati–Benioff zones based on the zones of high seismic activity (Isacks and Barazangi, 1977; Jarrard, 1986; Giardini and Woodhouse, 1984; Giardini, 1992; Lundgren and Giardini, 1992; Sugi et al., 1989; Engdahl et al., 1998) and the results of seismic tomography (van der Hilst et al., 1991; Fukao et al., 1992; Ding and Grand, 1994; Grand, 1994; van der Hilst, 1995; Engdahl et al., 1995; Sakurai, 1996; van der Hilst et al., 1997; Bijwaard et al., 1998) to define the deformation of slabs. These two methods are complementary. The Wadati–Benioff zones represent zones of high seismicity and can be correlated with cold descending lithospheric slabs. Errors in focal positions after relocation are ∼10 km or less and therefore maps of focal positions provide high resolution three-dimensional images of seismogenic regions (slabs) (Engdahl et al., 1998). However, these data are limited to the portions of slabs that have high seismicity and hence no constraints can be placed from the morphology of Wadati–Benioff zones where deformation is aseismic, such as below the 660 km discontinuity. Seismic tomography can provide insights into slab morphology, including aseismic regions, although its resolution is much worse than that of the Wadati–Benioff zones.

Fig. 1 shows two-dimensional morphologies of a section of some subducted slabs. Although, in reality, slabs deform in three-dimensions (Yamaoka et al., 1986), we choose several portions of slabs that show approximately two-dimensional deformation to facilitate comparison with our two-dimensional model. Because we focus on slab deformation in the transition zone, only the geometry of Wadati–Benioff zones below 200 km depth is considered. Several points can be noted. (1) Most of the slabs above ∼400 km depth are nearly straight (or planar) implying a high rigidity. (2) In several slabs (Izu–Bonin, Banda and Tonga, etc.), significant deformation occurs near the bottom of the transition zone. (3) However, slabs in South America and Honshu (not shown here) are planar close to the 660 km discontinuity, suggesting relatively high strength. (4) The Tonga slab shows significant deformation not only toward the bottom of the transition zone, but also around ∼400 km depth. Deformation at this depth is concentrated at ∼21°S–178°E and is highly three-dimensional.

The deformation that occurs at around 400 km depth in the Tonga slab is anomalous for several reasons: (i) the focal mechanisms of deep earthquakes in that region are significantly different from those of surrounding regions (Giardini, 1992; Giardini and Woodhouse, 1984); (ii) this region corresponds to the extension of the Louiville ridge which has thicker than normal oceanic crust (Vogt et al., 1976); and (iii) the deformation of this region may be related to the opening of the Lau basin to its north-west (Isacks and Barazangi, 1977). Therefore we focus on the first three of the above points in this paper. We also observe significant regional variations in slab deformation. For example, pronounced deformation near the bottom of the transition zone is well documented in the Izu–Bonin and Banda subduction zones but not in the Mariana slab. Although the data are limited, the deep seismic zones under South America show much less deformation (Lundgren and Giardini, 1992). Therefore there is significant variation in slab deformation behavior. We will return to this point in the next section where observations from seismic tomography are summarized.

One of the most remarkable observations from high resolution tomography (van der Hilst et al., 1991; Fukao et al., 1992; Ding and Grand, 1994; Grand, 1994; van der Hilst et al., 1997; Bijwaard et al., 1998) is that there is a variety of styles of slab deformation:
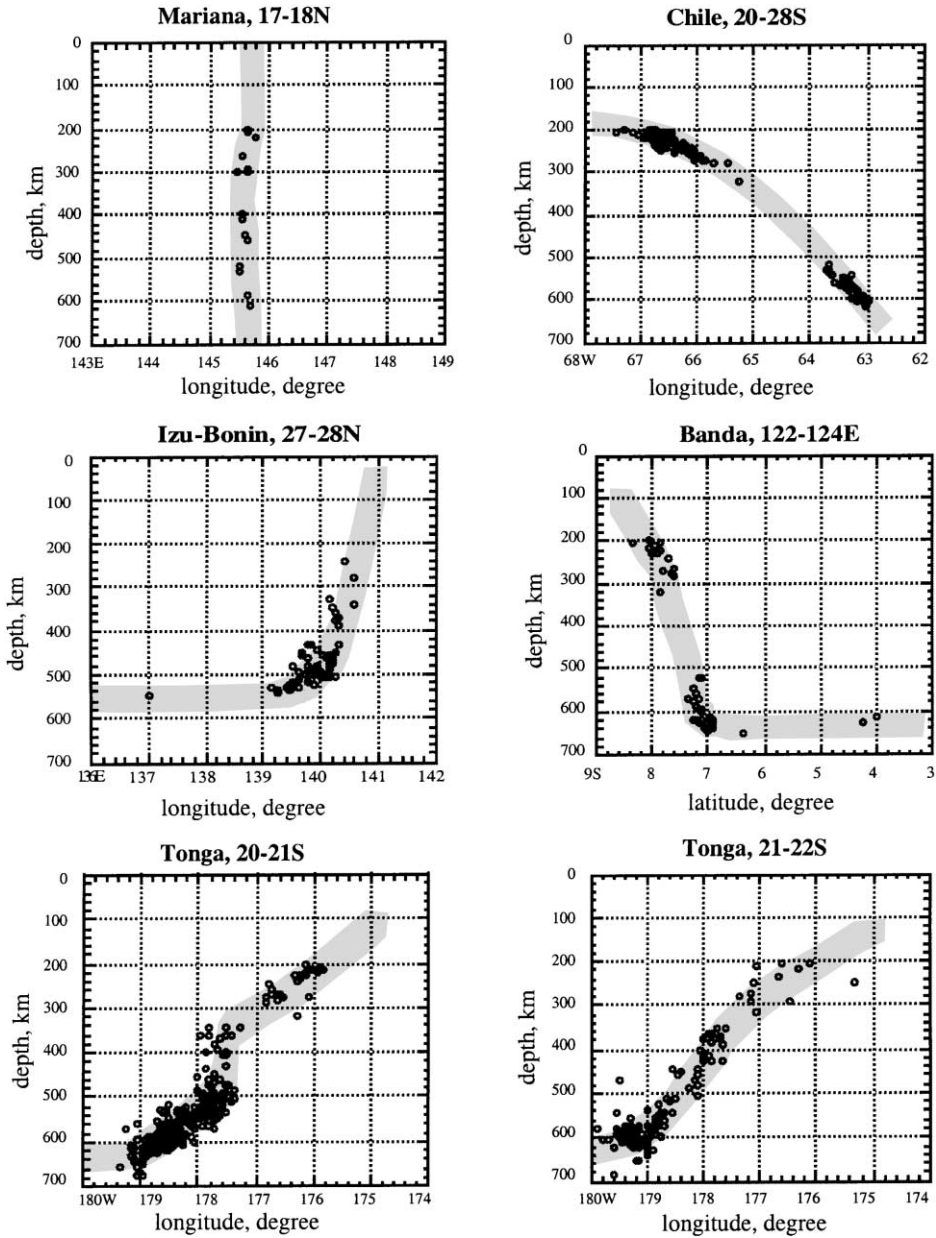
Fig. 1. Morphology of slabs (below 200 km) as inferred from distribution of earthquakes and from seismic tomography. Refined source locations by Engdahl et al. (1998) and tomographic results (van der Hilst et al., 1991; Fukao et al., 1992; van der Hilst, 1995; Sakurai, 1996; Bijwaard et al., 1998) are used. Each dot indicates a hypocenter (with a precision better than 10 km). Morphology of slabs in seismogenic regions is well constrained by hypocenter distribution. In general, slabs show little evidence for deformation from ∼200 to ∼400 km depth. Morphology in aseismic regions can only be inferred from tomographic images. Hatched regions show high velocity regions corresponding to subducted slabs inferred from seismic tomography. The shape and thickness of these regions are only poorly constrained. However, horizontal deflection of high velocity anomalies at around 600 km depth in the Izu–Bonin, Banda and Tonga is a robust feature of all high resolution tomographic studies. In contrast, no evidence for significant deformation is found in slabs in Americas and Mariana. Note a sharp change in slab morphology with a small change in latitude (i.e. three-dimensional morphology) in Tonga, which is presumably caused by the subduction of a buoyant ridge (Vogt et al., 1976) or by the opening of the Lau basin (Isacks and Barazangi, 1977).

in some regions such as Izu–Bonin, Banda and southern Kurile, the slabs show significant deflection at the 660 km discontinuity where they lie nearly horizontally. The best example is the Izu–Bonin slab which lies horizontally over a distance of more than 2000 km. In these areas, images of slabs in the lower mantle are poorly resolved although fast regions near the bottom of the mantle suggest that slabs do reach the bottom eventually. The lack of clear images of slabs in the lower mantle may indicate that the sinking velocity in the lower mantle is fast presumably because subduction into this region occurs only after the accumulation of a large amount of material on top of the 660 km discontinuity ("flushing events"; Honda et al., 1993; Tackley et al., 1993). In other regions, including beneath Americas and Tethys, continuous images of slabs can be observed more or less following the trend in the upper mantle, suggesting much less deformation of slabs in the transition zone.

2.1. Classification of slab deformation

The high resolution images of the Wadati–Benioff zones and the relatively low resolution images from seismic tomography both strongly suggest that there are two classes of slabs: (1) (type A) slabs that penetrate directly into the lower mantle without much deflection in the transition zone. Slabs under the Americas, north Kurile, Java and Kermadec belong to this category. The slab in the Mariana (and perhaps in the Kermadec) subduction zone appears to penetrate deep into the lower mantle, but the slab image becomes broad in the lower mantle suggesting significant deformation in this region; and (2) (type B) slabs that are significantly deflected above the 660 km discontinuity. The slab in the Izu–Bonin subduction zone is the best example. The Tonga slab is another example, although the horizontal extent of the slab deflection is not as large as that in Izu–Bonin. The New Guinea, south Kurile and Japan slabs are also examples of this type. The degree of deformation of slabs in the Americas is difficult to estimate because of poor resolution. Regional tomography by Engdahl et al. (1995) suggests some deformation but the geometry is poorly constrained. It is obvious, however, that the degree of slab deformation near the 660 km discontinuity in these subduction zones is significantly less than under the western Pacific.

A wider variety of deformation behavior has been observed from laboratory experiments (Griffths et al., 1996; Guillou-Frottier et al., 1996), numerical modeling (Christensen, 1996) and Wadati–Benioff zone morphology (Giardini and Woodhouse, 1984; Jarrard, 1986; Giardini, 1992; Lundgren and Giardini, 1992). However, we adopt this simple classification, because the main issue in this paper is the deformation of slabs at around the 660 km discontinuity; in addition the limited resolution of current seismic tomography does not justify further sophistication.

Styles of slab deformation may be related to the various parameters of subduction. First, the age and velocity of subducting lithosphere will control deformation behavior through their effects on temperature which affects both slab strength and the buoyancy forces. Wortel and Vlaar (1988) suggested a slab thermal parameter defined by $\Phi = tv_{\mathrm{sub}}$ (t: age of lithosphere at the time of subduction, v_{sub}: velocity of subduction) to characterize the minimum temperature of slabs. Second, trench migration velocity (Olbertz et al., 1997), v_{m}, may influence the deformation behavior of slabs as suggested by laboratory studies (Griffths et al., 1996; Guillou-Frottier et al., 1996) and by numerical modeling (Christensen, 1996). We estimated the slab thermal parameters and trench migration velocities, using a compilation of current subduction parameters (Olbertz, 1997) and subduction history (Lithgow-Bertelloni and Richards, 1998). Values of v_{m} and v_{sub} and morphology of slabs according to the above classification are summarized in Table 1.

Fig. 2 summarizes the correlation among slab deformation and subduction parameters. Note that in estimating the trench migration velocity and the slab thermal parameter, we choose the data corresponding to the slab properties from the surface to around 660 km depth. This is done because the geometry of slabs near the 660 km discontinuity in the transition zone is considered to be determined by the properties of slabs in that region of the mantle and the kinematic boundary condition, such as the trench migration velocity, during the period when a slab interacts with the 660 km discontinuity. For example, for a slab in the Izu–Bonin subduction zone, the latter corresponds to a period from ∼10 million years ago to the present.

Several points can be noted from Fig. 2. First, despite an earlier claim (van der Hilst and Seno, 1993),

Table 1
Classification of slabs and subduction parameters[a]

Name	Type	v_m (cm per year)[b]	v_{sub} (cm per year)[c]	Age (million years)	Φ (km)[d]
North Kurile	A	1	7.3	120	8760
South Kurile	B	1	8.7	130	11300
Northeast Japan	B	0.7	9.6	130	12480
Izu–Bonin	B	3.7	8.7	146	12700
Mariana	A	1.2	9.5	155	14725
Java	A	0.5	7.7	96–134	7400–10300
Banda	B	–	8.1	150	12150
New Guinea	B	1.0	7.0	–	–
Tonga	B	4.2	9.9	113	11200
Kermadec	A	1	8.9	98	8720
South Chile	A	2.8	4.4	26	1140
Central Chile	A	3.1	4.4	48	2110
North Chile	A	3.4	4.5	82	3690
Peru	A	3.1	3.7	45	1670
Central America	A	1.4	5.7	23	1311
North America	A	1.3	–	0–5	–

[a] Data of v_m, v_{sub} are from the compile by Olbertz (1997) and Lithgow-Bertelloni and Richards (1998). Classification of slab deformation is based on the shape of the Wadati–Benioff zone from deep seismicity (Engdahl et al., 1998) and the results of seismic tomography (van der Hilst et al., 1991; Fukao et al., 1992; van der Hilst, 1995; Sakurai, 1996; Bijwaard et al., 1998).

[b] v_m: trench migration velocity.

[c] v_{sub}: velocity of subduction.

[d] Φ: slab thermal parameter (age × v_{sub}).

the local variation in slab deformation behavior does not show a clear relation with the trench migration velocity. Sharp changes in slab geometry observed in the Izu–Bonin–Mariana, northern to southern Kurile and in the Tonga–Kermadec subduction zones do not correlate with the variation in the trench migration velocity. In the Izu–Bonin–Mariana subduction zone where the most dramatic change in the style of slab deformation occurs, the trench migration velocities have remained similar in each region from ~10 million years ago to the present, although there was a significant variation between 30 and 17 million years ago due to the opening of the Shikoku basin (van der Hilst and Seno, 1993). Similarly, the change in the style of subduction from the northern to southern Kurile (Fukao et al., 1992; Ding and Grand, 1994) does not have an obvious relation to trench migration. Note also that in the Tonga–Kermadec trench, very significant trench migration is observed from ~50 million years ago to the present (Lithgow-Bertelloni and Richards, 1998). Yet, no significant slab deflection is observed in the Kermadec subduction zone. Furthermore, in the Americas where trench migration, similar to that of some of the western Pacific subduction zones occurs, evidence for

slab deformation is less than that in the western Pacific. Thus, the correlation between trench migration and slab deflection appears rather indirect and weak. Second, there is a broad correlation between the slab thermal parameters and slab deformation: all the slabs with significant deformation around the 660 km discontinuity are in the western Pacific and have high slab thermal parameters, which indicate low temperatures and/or high subduction velocities.

The rather dramatic local variations observed in slab geometry suggest that deformation of a slab is controlled to a large extent by the local force balance and/or local tectonic history (kinematic boundary conditions). Thus, factors controlling slab deformation may be sought in some local parameters rather than global circulation, although global circulation certainly has an important effect on slab geometry (e.g. Hager and O'Connell, 1978). Based on the weak correlation between the observed trench migration and slab deformation, we consider that the role of trench migration in slab deformation is secondary. In contrast, the difference in the style of deformation between slabs with large and small thermal parameters seems more fundamental.
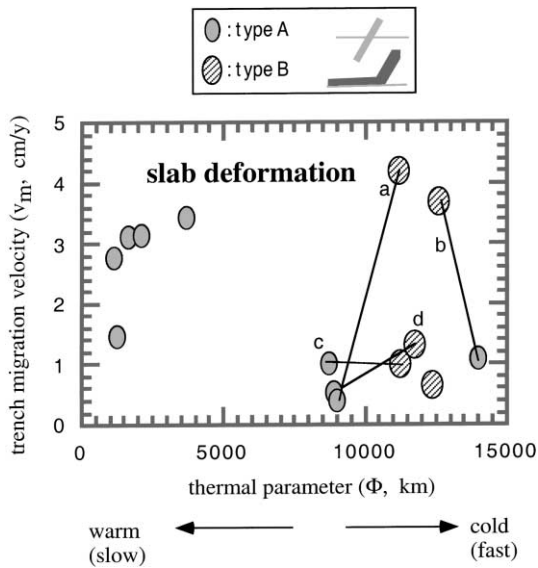
Fig. 2. Correlation of style of slab deformation with the slab thermal parameter Φ and trench migration velocity v_m. Slab geometry is classified into two categories (types A and B). The data are summarized in Table 1. Ages and kinematic data are the average values from the surface to the 660 km discontinuity. Portions of slabs that are connected are indicated by a tie line. Note a general correlation that type A behavior (direct penetration of slabs into the lower mantle without much deformation) occurs mostly for slabs with small thermal parameters and type B behavior (significant deformation above the 660 km discontinuity) occurs mostly for slabs with large thermal parameters. Correlation of deformation behavior with trench migration velocity suggested by previous studies (van der Hilst and Seno, 1993) appears secondary. An exception is the slab at the Mariana trench, which has the largest thermal parameter, yet penetrates into the lower mantle without much deformation above the 660 km discontinuity. The reason for this exception may be its very steep dip angle ($\sim 90°$) which results in a small bending moment ((a) Tonga–Kermadec; (b) Izu–Mariana; (c) Java–Banda; (d) Kurile–Japan).

Other sets of observations on slab deformation or rheology include: (i) the geoid anomalies around the subduction zones of western Pacific (Moresi and Gurnis, 1996; Zhong and Davies, 1999); (ii) the magnitude of stress drops of deep earthquakes (Kanamori and Anderson, 1975; Sugi et al., 1989; Kikuchi and Kanamori, 1994); and (iii) a sudden steeping of slab dip angle at the seismicity cutoff (Castle and Creager, 1998). The analysis of geoid anomalies in the western Pacific suggests that slabs there are weak and only little stress is transmitted along the slabs.

In addition, stress drops associated with deep earthquakes in the Tonga subduction zone (Sugi et al., 1989) are ~ 80 MPa, which are higher than those associated with the shallow earthquakes (Kanamori and Anderson, 1975), but not as high as would be expected if the slab stress is determined by viscosity that depends only on temperature and pressure. Note also, however, that the stress drop associated with the Bolivia deep earthquake of 1994 is significantly higher (~ 110 MPa) than those of Tonga (Kikuchi and Kanamori, 1994). All of these observations, taken together, strongly suggest that deep slabs, particularly those in the western Pacific, are rather weak. Similarly, the results of numerical modeling of slab deformation are consistent with the observations of slab morphology and focal mechanisms of deep earthquakes only when a rather weak temperature-dependence of rheology is assumed (e.g. Zhong and Gurnis, 1995).

These observations indicate that: (i) a slab with a large thermal parameter (low temperature and/or high subduction rate) is easier to deform than those with smaller thermal parameters; and (ii) a high rate of trench migration favors slab deformation (or flattening above the 660 km discontinuity) but its effect is rather indirect. Therefore we suggest that variation in the slab rheology through the variation in the slab thermal parameters may play an important role in controlling the style of slab deformation. However, the above observations imply a seemingly strange temperature dependence of slab strength: a cold slab appears to be weaker than a warm slab. To solve this paradox, we need to investigate the relation between slab rheology and its deformation and the dependence of slab rheology on temperature under conditions characteristic of the deep transition zone.

3. Slab deformation and rheology

3.1. Deformation of subducted slabs

Deformation of subducted slabs in the transition zone may occur for a number of reasons. First, when the trench migration velocity is significantly higher than the terminal velocity of a slab in the lower mantle (due to a high viscosity there), then slabs will be deformed above the 660 km discontinuity to lie horizontally above it *if they are weak* (Griffths et al., 1996;

Christensen, 1996; Olbertz et al., 1997). Second, slab deformation may occur due to the resistance forces exerted by the 660 km discontinuity, for example, the buoyancy forces caused by the phase transformation(s) that occurs at around the 660 km discontinuity (Tackley, 1997) or by an increase in viscosity (Gurnis and Hager, 1988). The presence of resistance forces deep in the transition zone has been documented by the focal mechanisms of deep earthquakes (e.g. Isacks and Molner, 1969). In both cases, the balance of the moment caused by the external forces acting at/or around the 660 km discontinuity and the bending moment due to the strength of the deforming slab materials determines the extent of slab deformation. For slabs in the deep transition zone, contribution from elastic stress is relatively small and therefore the moment balance equation is (Turcotte and Schubert, 1982)

$$M = \int_{-h/2}^{h/2} \sigma y \, \mathrm{d}y = -4 \int_{-h/2}^{h/2} \eta \dot{\varepsilon} y \, \mathrm{d}y \tag{1}$$

where h is slab thickness, σ and $\dot{\varepsilon}$ the longitudinal stress and strain-rate in a slab, y the distance from the center of the slab (Fig. 3), M the bending moment caused by the external forces and η the effective viscosity defined by $\eta = -\sigma/4\dot{\varepsilon}$ which generally depends on strain-rate (or stress), grain-size, temperature and pressure.
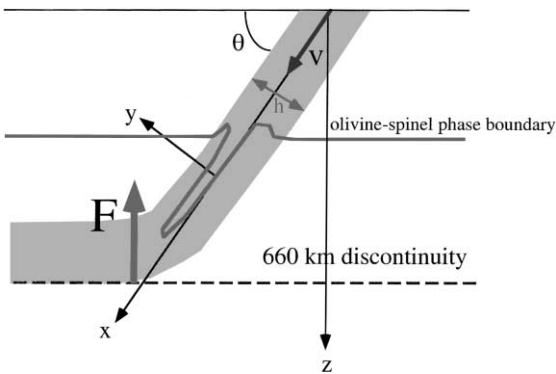
Fig. 3. Definition of the coordinate system. A slab encounters a barrier at the 660 km discontinuity which exerts a force in the vertical direction. The force due to this barrier provides a bending moment to the slab which tends to bend the slab. The degree of slab deformation depends on its rheological properties which depend on temperature, the magnitude of force (F) and subduction geometry such as the dip angle (θ).

For simplicity we assume that $\dot{\varepsilon} = \dot{\varepsilon}_0 y/h$, where $\dot{\varepsilon}_0$ is twice the strain-rate at the slab surface. Thus

$$M = \frac{\dot{\varepsilon}_0 D(\dot{\varepsilon}_0)}{h} \tag{2}$$

where we define D (flexural rigidity which has the dimensions of Nms) as

$$D \equiv 4h^3 \int_{-1/2}^{1/2} \eta(\dot{\varepsilon}) y'^2 \, \mathrm{d}y' \tag{3}$$

For a case of uniform linear rheology, D is independent of $\dot{\varepsilon}_0$ and $D = h^3 \eta/3$. However, for a more general case of non-linear and inhomogeneous rheology, Eq. (2) is an implicit equation that can be used to determine $\dot{\varepsilon}_0$ and hence D. Thus, Eq. (2) must be solved numerically by iteration using appropriate constitutive relations for slab materials. Note that the assumption of $\dot{\varepsilon} = \dot{\varepsilon}_0 y/h$ leads to an upper bound for a realistic value of D. More heterogeneous deformation would yield a smaller D. To solve Eq. (2) we need to know both the relevant rheological constitutive relation and $M(x)$. However, since the depth variation of rheological properties is significantly larger than that of $M(x)$ (for discussions on the depth variation of $M(x)$, see Bina, 1996, 1997; Yoshioka et al., 1997; Schmeling et al., 1999), we make a simplifying approximation that $M(x)$ is independent of x. Using this assumption, we can solve Eq. (2) to determine $D(x)$.

The forces acting on a slab at/or around the 660 km discontinuity include the forces due to the density anomalies caused by the deflection of the 660 km discontinuity (Tackley, 1997; Schmeling et al., 1999), forces due to the density anomalies caused by the buoyancy forces associated with subduction of a garnetite layer (Ringwood and Irifune, 1988; O'Neill and Jeanloz, 1994) and the resistance forces due to a high viscosity of the lower mantle. All of these forces increase with the velocity of subduction (and with the age of the lithosphere). For simplicity, we assume a linear relation between the moment M and the velocity of subduction. We choose bending moments of $M = 4 \times 10^{18}$ and 9×10^{18} N for velocities of 4 and 10 cm per year, respectively, which corresponds to a force of $F \sim 10^{13}$ N m^{-1} (Davies, 1980). It must also be noted that the bending moment due to external forces depends on the dip angle: for a large dip angle the bending moment is small.

The curvature of a slab may also be calculated from the slab strain-rate calculated above. From the definition of curvature $1/R = \mathrm{d}^2 w/\mathrm{d}x^2$ (where R is the radius of curvature, w displacement normal to the surface of the slab), and the relation $\dot{\varepsilon} = -y(\mathrm{d}^3 w)/(\mathrm{d}^2 x\, \mathrm{d}t)$ (Turcotte and Schubert, 1982), one can write

$$\frac{\dot{\varepsilon}_0}{h} = \frac{\mathrm{d}(1/R)}{\mathrm{d}t} \approx v_{\mathrm{sub}} \frac{\mathrm{d}(1/R)}{\mathrm{d}x} \tag{4}$$

where v_{sub} is the velocity of subduction. Note that we assume a steady-state shape of the slab. Thus, given $\dot{\varepsilon}_0(x)$ one can integrate Eq. (4) to obtain the radius of curvature of the slab $R(x)$.

The flexural rigidity, D, is sensitive to the rheological properties of slab materials, which change with both depth and lateral position due to changes in temperature, stress, pressure and grain-size. Slab temperatures depend on a number of factors including the initial temperature profile before subduction which depends on the age of the slab, thermal conduction and the latent heat release associated with phase transformations. We use a model similar to that of McKenzie (1969) with the additional effects of latent heat release (Riedel and Karato, 1997). We consider slabs with different initial thicknesses from 60 to 100 km which correspond to ages of ∼60–180 million years at the beginning of subduction. Here we show the results of detailed calculation for an initial thickness of 85 km with subduction velocities ranging from 4 to 10 cm per year. The range of parameters considered thus covers slab thermal parameters ranging from 2560 to 17,700 km.

3.2. Rheology of subducted slabs

3.2.1. Mineral physics considerations

To solve Eq. (2) with (3), we need to know the rheological properties of materials composing a slab. The rheological properties of subducting slabs can change both laterally and radially, because a number of parameters that affect rheology (temperature, pressure, stress and grain-size, etc.) can change both laterally and radially. In this paper, we will make the following simplifications. (1) We assume that the rheology of a subducting slab is controlled by its major component, $(Mg, Fe)_2SiO_4$, because this component is volumetrically dominant (e.g. Ringwood, 1991) and its rheology is usually softer than other components such as $(Mg, Fe)SiO_3$ (e.g. Karato, 1989a, 1997b). A thin strong garnetite layer may play an important role in the chemical evolution of slabs (Karato, 1997a), but its effects on the overall strength of slabs are not very large and will therefore be neglected in this paper. (2) Major phase transformations that may occur in $(Mg, Fe)_2SiO_4$ in the transition zone include olivine to wadsleyite, wadsleyite to ringwoodite (spinel) and olivine to ringwoodite. However, to simplify the analysis, we assume that only one transformation occurs in $(Mg, Fe)_2SiO_4$ in subducting slabs. We assume an equilibrium boundary corresponding to that of the olivine to wadsleyite transformation (e.g. Akaogi et al., 1989) and use the kinetic parameters for the olivine to spinel transformation from the experimental work by Rubie et al. (1990) on Ni_2SiO_4 to calculate the depth of transformation and the degree of grain-size reduction (for details, see Riedel and Karato, 1997). This admittedly crude approximation is made firstly because the behavior of wadsleyite in phase transformation appears similar to that of ringwoodite (Rubie and Ross, 1994) and secondly because detailed quantitative data on transformation kinetics are available only for the olivine to spinel transformation in Ni_2SiO_4 (Rubie et al., 1990; for a new data set on $(Mg, Fe)_2SiO_4$, see Mosenfelder et al., this volume). We believe that the essence of our model, i.e. semi-quantitative conclusions concerning the weakening of slabs and the effects of slab temperature on rheology, are not seriously affected by these simplifying assumptions.

Under these assumptions, we can characterize the rheology of a slab by knowing the rheology of olivine and ringwoodite, as well as knowing how the olivine to ringwoodite transformation affects rheology. We consider three deformation mechanisms, namely, power-law dislocation creep, diffusion creep and the Peierls mechanism. The rheology of olivine (Karato et al., 1986; Hirth and Kohlstedt, 1995a,b), wadsleyite (Kubo et al., 1998a; Mosenfelder et al., 2000; see however, Chen et al., 1998) and ringwoodite (Chen et al., 1998) is likely to be affected by water. However, we will consider rheology under water-free conditions, because oceanic lithosphere is considered to be depleted in water due to partial melting at mid-oceanic ridges (Karato, 1986; Hirth and Kohlstedt, 1996; Karato and Jung, 1998).

For olivine, we use the parameters determined by Evans and Goetze (1979), Karato et al. (1986),

Karato et al. (1993), Hirth and Kohlstedt (1995a,b) and Karato and Rubie (1997). The rheology of ringwoodite is less well constrained than that of olivine. However, a deformation mechanism map has now been constructed by the combination of direct mechanical tests on ringwoodite under transition zone conditions (Karato et al., 1998) and high resolution mechanical tests on analog spinels at lower pressures (Okamoto, 1989; Lawlis et al., 2001). In addition, the strength of ringwoodite (and wadsleyite) in the high stress, Peierls mechanism regime is constrained by the experimental data (Chen et al., 1998; Mosenfelder et al., 2000) together with the scaling law (Frost and Ashby, 1982). These data provide constraints on the degree of weakening caused by grain-size reduction resulting from the olivine–ringwoodite transformation.

A generic equation that describes the dependence of rheology on temperature, stress and pressure is given by

$$\dot{\varepsilon} = A \left(\frac{\sigma}{\mu} \right)^n \left(\frac{b}{d} \right)^m \exp \left[-g \frac{T_m(P)}{T} \left(1 - \frac{\sigma}{\sigma_P} \right)^q \right] \tag{5}$$

where A is a constant, σ the stress, μ the shear modulus, n the stress exponent, m the grain-size exponent, b the length of the Burgers vector, d the grain-size,

g a non-dimensional constant proportional to the activation enthalpy, T_m the melting temperature, T the temperature, P the pressure, σ_P the Peierls stress and q a constant that depends on the mechanism of dislocation glide (Frost and Ashby, 1982). One important assumption implicit in this formulation is that the pressure dependence of deformation can be parameterized through that of the melting temperature. The validity of this assumption has been evaluated by Weertman (1968), and Karato (1989a, 1997b, 1998) in particular showed that the melting temperature in this equation should be the melting temperature of constituent minerals as opposed to the solidus. We use the melting temperatures of major mantle minerals as compiled by Ohtani (1983) and Presnall and Walker (1993). Parameters in Eq. (5) used in this study are summarized in Table 2.

Important points to be emphasized are (1) due to the variation in stress in a slab, deformation mechanisms may change from low stress regions to high stress regions. In high stress regions, the Peierls mechanism will operate and this will limit the stress magnitude in these regions. (2) When grain-size reduction occurs due to a phase transformation, grain-size sensitive creep may operate. This will significantly reduce the strength when the degree of grain-size reduction is large. The degree of grain-size reduction depends on the temperature of a slab, as discussed below, and has

Table 2
Creep law parameters for olivine and spinel (ringwoodite)[a]

	A (s^{-1})	n	m	g	σ_P (GPa)	q
Olivine						
Peierls[b]	5.7×10^{11}	0	0	31	8.5	2
Power-law[c,d]	3.5×10^{22}	3.5	0	31	–	0
Diffusion[c,d]	8.7×10^{15}	1	2.5[e]	17	–	0
Spinel						
Peierls[f]	7×10^{11}	0	0	31	10	2
Power-law[g]	4×10^{22}	3.5	0	31	–	0
Diffusion[g]	2×10^{16}	1	2.5[e]	17	–	0

[a] A generic creep law formula of $\dot{\varepsilon} = A(\sigma/\mu)^n(b/d)^m \exp[-g(T_m(P)/T)(1 - (\sigma/\sigma_P))^q]$ is assumed ($T_m(P)$: melting temperature).
[b] Evans and Goetze (1979).
[c] Karato et al. (1986), Hirth and Kohlstedt (1995b) and Karato and Rubie (1997).
[d] Karato et al. (1986), Karato et al. (1993) and Hirth and Kohlstedt (1995a).
[e] Grain-size exponent (m) is assumed to be 2.5 considering the uncertainties involved in extrapolation (see Karato et al., 1986; Karato and Wu, 1993).
[f] Estimated from Chen et al. (1998) and a scaling law by Frost and Ashby (1982).
[g] Estimated from Karato et al. (1998) and Lawlis et al. (2001).

an important influence on the temperature dependence of rheology in such regions.

The effects of phase transformations on rheology were reviewed by Karato (1997b) and include: (1) intrinsic effects of change in crystal structure and chemical bonding; (2) transient effects of internal stress/strain; (3) transient effects caused by the change in temperature due to latent heat; and (4) transient effects through the change in grain-size. As far as the olivine to spinel transformation is concerned, the first factor (effects of crystal structure change) is not very large (Karato, 1989a, 1997b; Lawlis et al., 2001). The second mechanism, namely, "transformational plasticity" was suggested by Gordon (1971), Sammis and Dein (1974), Poirier (1982) and Panasyuk and Hager (1998), but there has been no convincing experimental demonstration of this effect on silicate minerals or their analogs (Meike, 1993; Zhao et al., 1999). Paterson (1983) proposed that recovery would reduce this effect and this mechanism will not be effective at least in warm regions (say $T > 1300$ K). Recent experimental data on dislocation recovery in olivine under deep upper mantle conditions (Karato et al., 1993) support this notion. Therefore, in this paper, we consider the effects of crystal structure change, effects of latent heat release and the effects of grain-size reduction on rheology and ignore the effects of internal stress/strain.

Vaughan and Coe (1981) first suggested the possible importance of grain-size reduction associated with mantle phase transformations on mantle rheology. Rubie (1984) elaborated this idea and discussed the causes of regional variation in dynamics of deep slabs as related to the olivine–spinel transformation. However, none of these early works provided a quantitative estimate of these effects and, even qualitatively, the effects of temperature were not appropriately included because data on transformation kinetics and rheology of high pressure phase(s) was not available and a quantitative theory for transformation kinetics had not been developed. Riedel and Karato (1997) presented the first quantitative calculation of grain-size and its effects on rheology associated with the olivine to spinel transformation. The essence of the model is that the grain-size of a new phase (spinel) after the transformation is determined by impingement and therefore by the balance of nucleation and growth (Axe and Yamada, 1986). In general, the grain-size, d, of a new

phase after the completion of a transformation and the time to complete the transformation, τ, are related to the kinetics of nucleation and growth as (Axe and Yamada, 1986; Riedel and Karato, 1996, 1997)

$$\tau \sim [Y(T, P)^{-k} I_k(T, P)]^{-1/(k+1)} \tag{6}$$

$$d \sim \left(\frac{Y(T, P)}{I_k(T, P)} \right)^{1/(k+1)} \tag{7}$$

respectively, where $Y(T, P)$ is the growth rate, $I_k(T, P)$ the nucleation rate and k a constant that depends on nucleation mechanism ($k = 2$ for inter-granular nucleation, $k = 3$ for intra-granular nucleation).

In a subducting slab, the characteristic time for phase transformation is largely controlled by the rate of subduction. It can be shown that under most conditions in subducting slabs (say $T > 900$ K for the olivine to ringwoodite transformation), the characteristic time is given by $\tau \sim \Delta L / v_{sub}$ (ΔL is the overshoot depth for transformation (an excess depth beyond the equilibrium depth needed for transformation), v_{sub} velocity of subduction, which is only weakly dependent on temperature (Riedel and Karato, 1997)). In this case, the temperature dependence of grain-size is controlled mostly by the temperature dependence of the growth rate. Consequently, the size of grains after the completion of a transformation tends to be small if the transformation occurs at low temperatures. Under these circumstances, the grain-size after the transformation depends on temperature as

$$d \sim Y\tau \propto \exp\left(-\frac{H_g^*}{RT} \right) \tag{8}$$

where H_g^* is the effective activation enthalpy that controls grain-size, which is close to the activation enthalpy for growth.

The rheological flow laws summarized in Table 2 show that when the spinel grain-size is less than $\sim 100\,\mu$m, then grain-size sensitive flow will dominate. In this case, the strain-rate depends on temperature as

$$\dot{\varepsilon} \propto \exp\left(\frac{mH_g^* - gRT_m(P)}{RT} \right) \tag{9}$$

where we assumed $q = 0$ for simplicity. For a typical range of parameters for mantle minerals, $mH_g^* - gRT_m(P) > 0$, which means that the effective activation enthalpy is negative and therefore the strain-rate
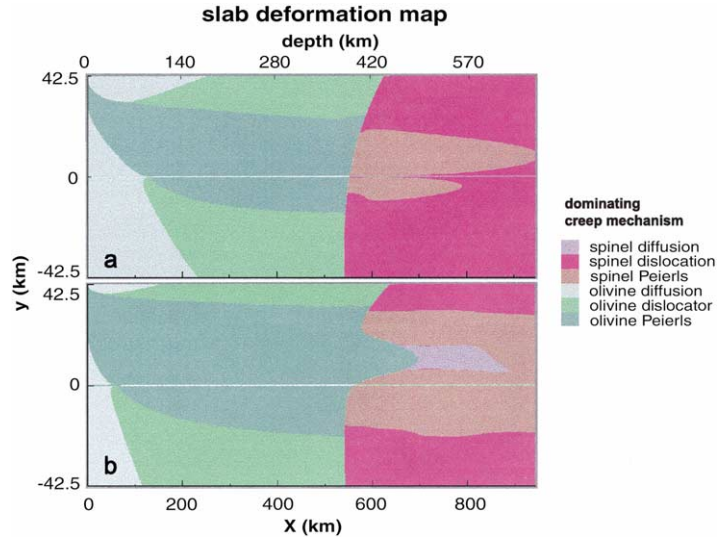
slab deformation map

Fig. 4. Dominant deformation mechanisms in subducting slabs. Initial temperature distribution corresponds to that for a 100 million years oceanic lithosphere of 85 km thickness. The cases for subduction velocities of (a) 4 and (b) 10 cm per year are shown. Because stress, temperature, pressure and grain-size change significantly in space for a given slab, dominant mechanisms of deformation change in a complicated fashion. In high stress, low temperature regions, the Peierls mechanism dominates. In moderate stress, moderate to large grain-size regions, power-law creep dominates. Diffusion creep plays an important role in cold, fine-grain regions in the center of slabs after a phase transformation. Note that such a pattern also depends on the velocity of subduction, which controls the temperature distribution and the magnitude of stress.
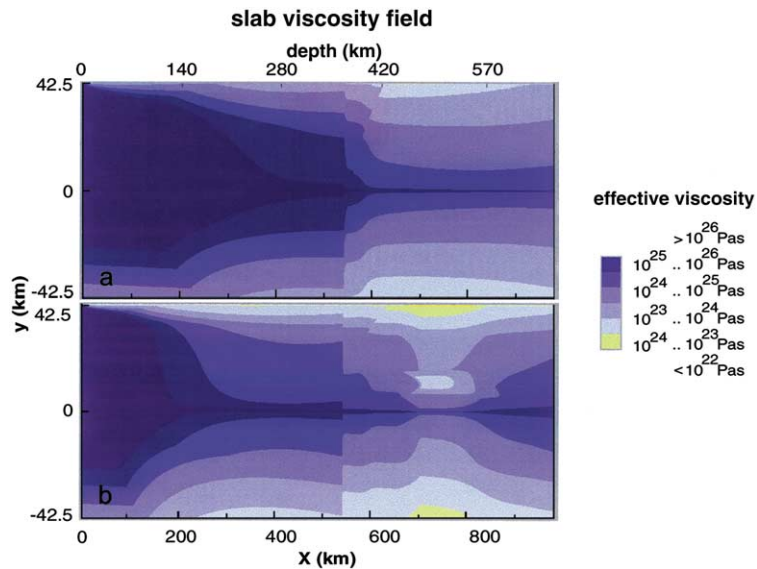
slab viscosity field

Fig. 5. Distribution of effective viscosity in subducting slabs corresponding to the cases shown in Fig. 4: (a) for $v_{sub} = 4$ cm per year and (b) for $v_{sub} = 10$ cm per year. Note that the center of the slab has high viscosities for 4 cm per year (a), but the central portions in the deep part of a slab for 10 cm per year (b) has low viscosity after the phase transformation because of small spinel grain-size. This low viscosity region recovers its strength due to progressive grain-growth at a greater depths.

will be *larger* for *lower* temperatures. This unusual behavior comes from the strong temperature dependence of grain-size after a phase transformation.

After the completion of a phase transformation, we use the grain-growth law to estimate the increase in grain-size. The kinetics of grain-growth have been investigated for olivine (Karato, 1989b), but a detailed data set on high pressure polymorphs is not available. In this study, we used preliminary data on grain-growth kinetics in wadsleyite studied at transition zone conditions ($T = 1473–1873$ K, $P = 16$ GPa; Karato, unpublished data) and assume that the kinetics of grain-growth in ringwoodite are the same as those in wadsleyite. We assume a canonical

form of grain-growth kinetics (see Karato, 1989b)

$$d^2(t) - d^2(0) = k_0 \exp\left(\frac{-H_{gg}^*}{RT}\right) t \qquad (10)$$

where $d(t)$ is grain-size at time t, H_{gg}^* the activation enthalpy for grain-growth (~ 500 kJ/mol) and k_0 the pre-exponential factor ($\sim 9 \times 10^3$ m^2/s). When a phase transformation occurs at low temperatures, small grains will survive for a long period. In contrast, when a phase transformation occurs at high temperatures, grain-growth is so fast that small grain-size will not survive for a long time. Thus, a slab will develop and maintain a significant weak fine-grained
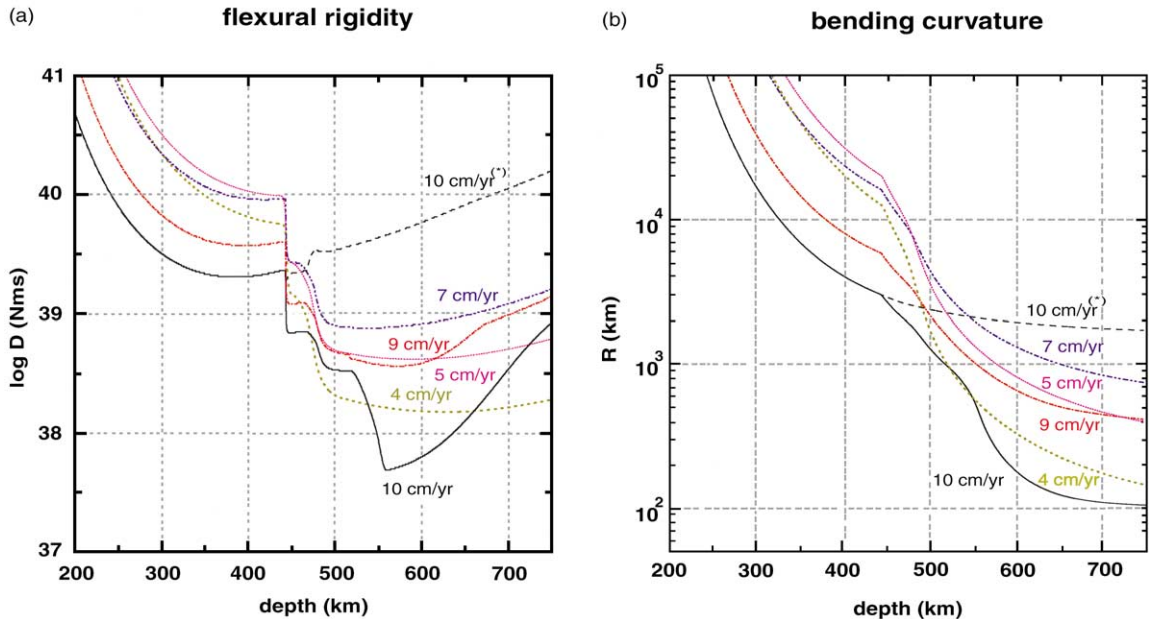

Fig. 6. (a) Flexural rigidity (D) vs. depth for slabs for various subduction velocities. An initial temperature distribution corresponding to oceanic lithosphere of 100 million years of age is used. The broken curve for 10 cm per year shows the results when the effects of latent heat release and grain-size reduction are ignored. Flexural rigidity generally decreases with depth due to the increase in temperature, and there is an abrupt decrease around 440 km due to the effect of latent heat release. In addition, the production of fine-grained spinel in the deep portions of fast slabs results in significant reduction in flexural rigidity. Velocity of subduction affects flexural rigidity through two different mechanisms. First, it affects flexural rigidity through the change in temperature (fast slabs are cold). Usually low temperatures result in high strength, but when the degree of grain-size reduction is large, strength will be low for low temperatures due to the large effect of temperature on grain-size. Second, velocity of subduction changes stress levels that also affect rheology. The second effect is important where the stress-sensitive Peierls mechanism dominates. The effects of grain-size reduction and of the stress magnitude on rheology result in a negative correlation between flexural rigidity and velocity of subduction. (b) Depth variation of radius of curvature. The broken curve for 10 cm per year shows the results when the effects of latent heat release and grain-size reduction are ignored. Steady-state deformation is assumed and the radius of curvature at 200 km is assumed to be infinite. The radius of curvature decreases significantly with depth due to rheological softening.

region only when a phase transformation occurs at low temperatures.

3.2.2. Slab rheology models

The calculation of flexural rigidity and rheological structure is made as follows. First, we assume a certain initial temperature profile for a slab corresponding to a certain age of subduction. A standard error function geothermal model of oceanic lithosphere is used (Turcotte and Schubert, 1982). We solve the equation for thermal conduction incorporating the equation for the kinetics of the olivine–spinel transformation that includes the effects of latent heat. This provides a temperature distribution (e.g. Daessler et al., 1996; Riedel and Karato, 1997). The solution of these equations provides nucleation and growth rates at each point in the slab, from which we estimate the grain-size using the scaling law described by Riedel and Karato (1996). Given temperature, pressure and grain-size, we calculate viscosity corresponding to an assumed moment M and initially assumed strain-rate $\dot{\varepsilon}_0$ for three different deformation mechanisms. We choose the one that gives the lowest viscosity. Then the right-hand side of Eq. (2) is used to calculate $\dot{\varepsilon}_0$. This calculation is repeated until the calculated value of $\dot{\varepsilon}_0$ agrees with the initial value within a fraction of 10^{-5}.

The results of such calculations are shown in Figs. 4–6. Fig. 4 shows the dominant mechanisms of deformation for slabs with two different temperature distributions. Dominant mechanisms of deformation change in a complicated way as a function of subduction parameter and space. The Peierls mechanism is a dominant deformation mechanism in the central portions of slabs where temperature is low and stress is high. However, in cold slabs, the central portion will be replaced with fine-grained ringwoodite after the olivine–ringwoodite phase transformation, and diffusional creep dominates in that portion thus significantly reducing the viscosity. In general, outer warm regions of slabs deform by dislocation creep. Effective viscosity varies laterally and also with the velocity of subduction (Fig. 5). Flexural rigidity D generally decreases and hence the radius of curvature decreases with depth as a result of the increase in temperature (Fig. 6a). Flexural rigidity (radius of curvature) decreases abruptly at ~440 km deep due to the effects of latent heat release. However, the radius of curvature remains large until a slab subducts deeper than

~500 km (Fig. 6b). The effect of grain-size reduction is large for cold fast slabs and is important particularly in regions deeper than ~500 km.

The flexural rigidity or the curvature in the deep transition zone has an important influence on the interaction of the slab with the 660 km discontinuity. Fig. 7a and b shows the variation of flexural rigidity (or the radius of curvature) at 600 km depth as a function of subduction velocity. The slab flexural rigidity (radius of curvature) first increases with subduction velocity, but there is a peak in D at ~7 cm per year
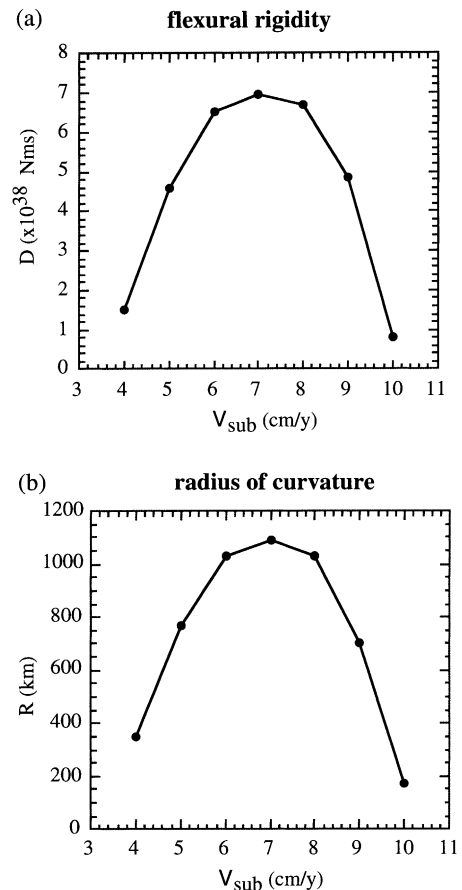

Fig. 7. The flexural rigidity D (a) and the radius of curvature (b) of subducted slabs at 600 km deep as a function of velocity of subduction. The rigidity and radius of curvature both increase with velocity in the range ~4–7 cm per year because of the decrease in temperature, but beyond ~8 cm per year, these parameters decrease with velocity of subduction mainly because of the effects of temperature on grain-size. Slabs are strongest at the intermediate velocities/temperatures.

and the flexural rigidity (radius of curvature) then decreases with subduction velocity at faster subduction velocities. Variation of the flexural rigidity (curvature) with the subduction velocity is partly due to the assumed increase in bending moment with subduction velocity. The sensitivity of slab rheology on the bending moment is discussed in Riedel et al. (1998) in detail. The bending moment can be modified by changing the force as well as the dip angle. A high dip angle near the 660 km discontinuity leads to a small bending moment.

We may note that the two trends shown in Figs. 5 and 7 can be seen clearly for the parameters (bending moment and initial thickness of the slab) that we choose. For other parameter sets, only one trend may be seen. For example, when one chooses much smaller initial thickness, then the slab temperatures are so high that the effects of phase transitions to reduce the slab strength are not seen clearly. The parameter set that we use here is chosen on the basis of geodynamical estimates (e.g. Davies, 1980) as well as mineral physics. The effects of change in parameters are explored in Riedel et al. (1998).

4. Discussion

4.1. Uncertainties in materials properties

4.1.1. Flow laws and grain-growth kinetics

Flow laws of olivine have now been well constrained at least under dry conditions (Karato et al., 1986, 1993; Hirth and Kohlstedt, 1995a,b, 1996). This includes the effects of pressure (Karato and Rubie, 1997) which are important under transition zone conditions. In contrast, flow laws for high pressure phases are still poorly constrained. The most critical points are the transition conditions that separates dislocation creep and grain-size sensitive creep and the flow law in the grain-size sensitive regime. However, due to an experimental study at transition zone conditions (Karato et al., 1998), we now have a constraint on the transition conditions between diffusion and dislocation creep in ringwoodite under laboratory conditions (the transition grain-size is $\sim 1\,\mu\text{m}$ at $\sigma/\mu \sim 10^{-2}$ and $T/T_\text{m} \sim 0.7$). To translate these conditions to geological conditions, we need to know flow law parameters particularly the stress exponents

and grain-size exponents. Flow law parameters in the grain-size sensitive regime currently have some uncertainties. Vaughan and Coe (1981) fitted their data for Mg_2GeO_4 spinel with a non-linear grain-size sensitive creep law ($n = 2$ and $m = 2$). However, a later systematic study on creep in spinels (Okamoto, 1989) demonstrated that diffusion creep ($n = 1$ and $m = 2$–3) or power-law creep ($n = 3$–4 and $m = 0$) dominates under most conditions. Our detailed study on germanate spinels also supports this conclusion (Lawlis et al., 2001). Therefore we used the flow law parameters for power-law creep and diffusion creep in this study for estimating the transition conditions to grain-size sensitive creep and estimate the transition grain-size under geological conditions ($\sigma/\mu \sim 10^{-3}$, $T/T_\text{m} \sim 0.4$–0.7) as $\sim 10^2$–$10^3\,\mu\text{m}$. Similar results on transition conditions between dislocation and diffusion creep have also been obtained in wadsleyite (Lawlis et al., 1999). Likewise, Chen et al. (1998) and Mosenfelder et al. (2000) noted a similarity in rheology between wadsleyite and ringwoodite in the low temperature plasticity regime (Peierls mechanism).

Uncertainties in grain-growth kinetics are large at this stage. To see the effects of uncertainties on the rheology of slabs in our models, we calculated the grain-sizes using different activation enthalpies by changing k_0 and H_gg^* simultaneously to satisfy the experimental constraints. A change in H_gg^* from 500 to 400 kJ/mol leads to only minor changes for a critical temperature for grain-growth ($\sim 80\,\text{K}$). We therefore conclude that the uncertainties in grain-growth kinetics will not significantly affect the main conclusions of this paper.

4.1.2. Transformation kinetics: effects of intra-granular transformation

Recently Rubie and his colleagues reported new mechanisms of phase transformation. Kerschhofer et al. (1996, 1998, 2000) found that the olivine to wadsleyite and olivine to ringwoodite transformations can occur through intra-granular nucleation as well as inter-granular (grain boundary) nucleation. Under some conditions, new phases are formed inside of old grains as opposed to at grain-boundaries, usually associated with stacking faults or dislocations. Such a new mechanism could modify the conclusions reached above, although the details of its effects are unclear, because quantitative details of the kinetics

of this mechanism have not been well constrained (some discussions on the kinetics of this process are given in Kerschhofer et al., 2000). We can make the following points.

1. In terms of the above analysis of grain-size evolution, the dependence of grain-size on temperature will be largely the same for both inter- and intra-granular nucleation mechanisms, because the temperature sensitivity of grain-size depends on the growth rate rather than the nucleation rate. Therefore one of the most important conclusions of our model, namely, the strong temperature dependence of grain-size after transformation will be valid even if this new mechanism operates.

2. The effects of intra-granular nucleation on rheology may be less dramatic than those of inter-granular nucleation, because the rheological effects of grain-size reduction depend strongly on the manner in which fine grained regions are connected (percolation transition). This percolation transition is easier for inter-granular nucleation than intra-granular nucleation (Riedel and Karato, 1996). Consequently, rheological weakening would occur at an earlier stage for inter-granular nucleation than for intra-granular nucleation.

3. Irrespective of the details, the operation of additional mechanisms will enhance transformation kinetics, so that the depth interval in which two phases coexist will be smaller.

In short, we consider that the recently-documented intra-granular nucleation mechanisms may modify the details of grain-size estimation, but the main conclusion on the temperature dependence of grain-size will not be modified significantly. However, the kinetic parameters relevant to intra-granular nucleation mechanisms have not been well constrained including the effects of stress (Mosenfelder et al., 2000). Therefore it is difficult to quantitatively discuss the effects of this mechanism at this stage.

4.1.3. Transformation kinetics: effects of transformation stress/strain

A first order phase transformation such as the olivine–spinel transformation is associated with a volume change. Consequently, plastic flow must occur to accommodate strain caused by the volume change. If untransformed material is completely surrounded by a strong material, then the volume change that occurs in that material results in a change in pressure that could prevent further transformation. Kubo et al. (1998b) and Mosenfelder et al. (2000) noted significant reduction in the growth rate of a new phase in the later stage of transformation and interpreted their results as caused by such an effect. However, the relevance of such observations on the phase transformation in a real slab is not clear, because the effect of plastic flow is dependent on the geometry of transforming materials. For a more general geometry of two phases, plastic flow to accommodate volumetric strain occurs mostly in a softer phase (olivine) (e.g. Greenwood and Johnson, 1965) and results in an increase in free energy of a weak phase. In such a case, the effects of plastic strain would *enhance* phase transformation rather than suppress it.

The effect of transformation stress/strain on the grain-size of newly formed spinel is not included in our model. However, a simple calculation shows that a change in free energy caused by plastic strain is usually significantly smaller than the difference in free energies between the two phases (olivine and spinel) and consequently the effects of transformation stress/strain on the grain-size of spinel will be small.

4.1.4. Effects of transformation strain-induced recrystallization

Rubie et al. (1998) also suggested that the strain-energy stored during a phase transformation might lead to grain-size reduction, a process analogous to dynamic recrystallization. Such a process is not considered in our model and could modify our conclusions. In principle, any additional mechanisms of grain-size reduction will further reduce the strength of subducting slabs. A key question is whether this new mechanism significantly modifies our main conclusion on the temperature dependence of rheology. Because the details of this process have not been analyzed, it is difficult to make any assessment of potential influence of this process at this stage. However, we can make some qualitative arguments. The size of grains formed by this process is determined by the competition between nucleation of "recrystallized" grains and their growth, similar to Eq. (7) (see Shimizu, 1998). The driving force for this type of recrystallization is dislocation energy which

is proportional to dislocation density. The higher the dislocation density, the smaller is the recrystallized grain-size. If one uses the assumption that the dislocation density after the transformation is determined by the volume change due to "geometrically necessary dislocations" as proposed by Poirier (1982), then the driving force is nearly independent of temperature. In this case, the temperature sensitivity of grain-size will depend mostly on the growth rate and hence the grain-size will be smaller when transformation occurs at low temperatures. In short, the effects of temperature on grain-size due to this mechanism is at least qualitatively similar to that of our model.

4.2. Comparison with previous studies

4.2.1. Effects of trench migration

Most of the previous models for slab deformation considered that the variation in trench migration velocities control slab deformation (van der Hilst and Seno, 1993; Griffths et al., 1996; Guillou-Frottier et al., 1996; Olbertz et al., 1997). However, this kinematic explanation has two major problems. First, such a kinematic model would work only when slab deformation is dynamically possible. In fact, all the experimental (Kincaid and Olson, 1987; Griffths et al., 1996; Guillou-Frottier et al., 1996) and theoretical modeling of slab deformation (Christensen, 1996; Olbertz et al., 1997) assumed low slab viscosities to make deformation possible. However, if deformability of slabs can vary from one slab to the other, then the effect of such variation must also be examined in addition to the influence of kinematic boundary conditions.

Second, the observational basis for inferring the importance of trench migration is not strong (Fig. 2). There is no obvious reason to suggest a causal relation between trench migration and slab deflection from the seismological observation and plate kinematics as discussed before. The contrast between western Pacific slabs (slabs with large thermal parameters) and those in the Americas (slabs with small thermal parameters) appears more fundamental. It is possible that the rapid trench migration observed in some of the western Pacific subduction zones could be a *result* of weak slabs and that the rapid trench migration is not the *cause* of deformation.

4.2.2. Effects due to the variation in buoyancy forces

Variation in buoyancy forces that control slab deformation may also be a cause of variation in slab deformation behavior. In our model, this is partly incorporated by assuming that the bending moment acting on a slab depends on subduction velocity. Such an effect has been analyzed by Bina (1996, 1997), Marton et al. (1999) and Schmeling et al. (1999) in more detail (also see Daessler et al., 1996). The pronounced bend observed in some slabs in the middle part of the transition zone (e.g. Tonga, see Fig. 1) might be due to the variation in buoyancy forces in addition to a change in rheology.

4.2.3. Deformation by earthquake faulting

The rheological models considered here assume homogeneous deformation. However, there is evidence for localized deformation in deep slabs. Several analyses suggest that some fraction of the strain in subducted slabs develops by seismic faulting (Sugi et al., 1989; Holt, 1995). In this case, the assumption of homogeneous rheology is not valid in its simplest form. However, deep earthquakes can explain only a part of the total strain. This is true particularly for the deep portions of slabs beneath the seismicity cutoff where the presence of weak slabs is inferred (Castle and Creager, 1998). Therefore, weak rheology in the ductile regime must play a significant role in many slabs.

Weakening in the ductile regime, where deformation is more or less homogeneous, may also be important for the generation of deep earthquakes. Many mechanisms of deep earthquake faulting are based on some form of rheological weakening (Hobbs and Ord, 1988; Green and Burnley, 1989; Kirby et al., 1991). In addition, the complicated rheological structures of deep slabs predicted by the present model suggest that deep earthquakes may originate in the deep slabs where high stress concentration occurs outside the regions of weak fine-grained spinel. This point will be discussed in more detail in Section 4.4.

4.2.4. Preexisting weak zones?

The presence of zones of weakness such as fossil fault planes might influence the deformability of slabs (Zhong and Gurnis, 1995; Silver et al., 1995). Such fossil fault zones may survive deep into the transition zone particularly in the cold portions of slabs. Fossil

fault zones may be weaker than other regions due to a small grain-size and/or to higher content of hydrous minerals (or higher content of hydrogen in nominally anhydrous minerals). Deformation along these zones may also contribute to slab deformation. However, it is not straightforward to explain the observed variations in the style of slab deformation by this mechanism, which would predict a positive correlation between seismicity at trenches and slab deformation in the transition zone. Such a correlation is not consistent with the observations (Engdahl et al., 1998).

4.3. Explanation of the variability of slab deformation behavior

How can we explain the diversity of slab deformation behavior by our model? First, our model provides a natural explanation for a puzzling observation that slabs with a large thermal parameter (i.e. low temperatures and/or fast subduction velocities) tend to be more prone to deformation. In our model, this occurs because of the strong temperature dependence of grain-size after the olivine–spinel transformation in addition to the higher stresses (bending moment) caused by a larger force. Obviously, if the slab temperature is very high, viscosity is too low and negative buoyancy forces are too small for penetration through the 660 km discontinuity. Over a reasonable range of slab temperatures, slabs with moderately high temperatures will have high enough strength to resist deformation near the 660 km discontinuity, whereas slabs with colder temperatures are weak enough to be significantly deformed. Thus, there will be a temperature range (a "window") in which slabs will be strong enough to penetrate through the 660 km discontinuity without much deformation (see Fig. 7). The 660 km discontinuity will act as a filter for slabs for rheological reasons. This provides a possible explanation for the observed correlation shown in Fig. 2. Among the slabs that are weak enough, the style of deformation will also depend on other factors including trench migration velocity and geometrical factors such as the dip angle.

4.4. Implications for deep earthquakes

Mechanisms of deep earthquakes have been reviewed in several recent papers (e.g. Frohlich, 1989;

Kirby et al., 1991, 1996; Green, 1994; Green and Houston, 1995; Karato, 1997b). Among others, the transformation faulting model has attracted much attention recently because experimental support for that model has been reported (Kirby, 1987; Green and Burnley, 1989; Kirby et al., 1991; Green et al., 1990; Tingle et al., 1993; Green and Zhou, 1996). Some of the seismological observations including the depth variation in deep earthquake activity (Frohlich, 1989) and spatial distribution of deep earthquakes (Wiens et al., 1993) appear to be consistent with this model if metastable transformations are assumed. However, some fundamental problems remain with this model (Karato, 1997b). The most serious difficulty with the transformational faulting model is that it predicts much smaller fault dimensions (10–20 km) for deep earthquakes than are observed (40–60 km) (Kikuchi and Kanamori, 1994; Wiens et al., 1994; Tibi et al., 1999). It is also uncertain if a metastable olivine wedge exists or not, particularly in relatively warm slabs such as those beneath South America. In addition, the recent observation of repeating deep earthquakes (Wiens and Snider, 1999) is difficult to reconcile with the transformational faulting model.

Furthermore, the processes of instability associated with phase transformations are not well understood. Most of the experimental studies on transformation faulting are on analog materials at low pressures (Green and Burnley, 1989; Kirby et al., 1991; Green and Zhou, 1996) where the magnitude of differential stresses is comparable to the confining pressure. Green et al. (1990) reported the occurrence of transformation faulting associated with the olivine–wadsleyite transformation in their experiments under the transition zone conditions. However, later studies in which deformation during pressurization is minimized by an improved sample assembly failed to reproduce transformation faulting under almost exactly the same conditions (Dupas-Bruzek et al., 1998; Karato et al., 1998). Furthermore, theoretical understanding of transformation faulting is inadequate. Most of the models are at best qualitative (Kirby, 1987; Green and Burnley, 1989; Kirby et al., 1991; Green, 1994), and a published quantitative model (Liu, 1997) contains an inappropriate use of the Levy-von Mises formulation of non-linear rheology in treating the interaction of internal stress and deformation which leads to a significant overestimate of this interaction. Therefore,

the only robust prediction from this model is that the fault plane is limited to the region where the phase transformation occurs and therefore the fault width should be less than 10–20 km (the expected width of the metastable olivine wedge). This prediction is obviously in contradiction to the observations of much grater fault widths, making this mechanism unlikely to be important.

Another model was proposed by Meade and Jeanloz (1991) who reported acoustic emissions associated with the dehydration and amorphization of serpentine under shallow and deep mantle pressures, respectively. They suggested that dehydration may cause intermediate earthquakes and amorphization could cause deep earthquakes. But this model for deep earthquakes has several difficulties. First and most important is that the recent high pressure, temperature experimental study on serpentine showed that the presumed amorphization does not occur under deep slab conditions (Irifune et al., 1996). Second, the physical mechanisms of instability have not been identified and therefore the scaling argument presented by Meade and Jeanloz (1991) is at best speculative. Therefore we consider that this model does not have strong support from mineral physics.

An alternative model for deep earthquakes is the thermal runaway instability (adiabatic instability) model originally proposed by Griggs and Baker (1969) and later elaborated by Ogawa (1987) and Hobbs and Ord (1988). Unlike the mechanisms discussed above, the physics of thermal runaway instability (adiabatic instability) is well understood both theoretically (Backofen, 1972; Poirier, 1980; Fressengeas and Molinari, 1987; Estrin and Kubin, 1988; Hobbs and Ord, 1988) and experimentally (e.g. Basinski, 1957, 1960; Backofen, 1972; Rogers, 1979; Staker, 1981). In addition, it has recently been demonstrated that the likely temperature dependence of thermal diffusivity under low temperature conditions significantly enhances thermal runaway instability particularly in spinel-rich regions (Branlund et al., 2000). Also, shear-induced melting in mantle rocks was documented in naturally-deformed mantle rocks from the Ivrea zone, northern Italy (Obata and Karato, 1995) and melting associated with the 1994 Bolivian deep earthquake was suggested (Kanamori et al., 1998). Therefore the thermal runaway model is worth special attention as a plausible cause of deep earthquakes. In

this section, we will first show that thermal runaway is likely to occur in deep slabs, and that this model, when combined with our model of rheological structures, provides a natural explanation for a large width of faults associated with deep earthquakes. We will then discuss some additional implications of this model.

The basic physics of thermal runaway instability is that when deformation of a material occurs rapidly enough in comparison with the time scale of thermal diffusion, heat is accumulated in the regions of high strain that further enhances the deformation; there is therefore a positive feedback between deformation-induced heating and deformation, leading to thermal runaway (Fressengeas and Molinari, 1987; Estrin and Kubin, 1988). When the stiffness of the surrounding system is not too high, then this leads to a runaway instability causing earthquakes (Hobbs and Ord, 1988). Therefore the key issues in thermal runaway are (i) the rate of deformation must be fast and (ii) the degree of thermal feedback must be large.

We use the model proposed by Hobbs and Ord (1988) for the onset of instability, but use a more realistic rheology to evaluate the plausibility of the thermal runaway instability model. For power-law creep, the condition for thermal runaway (adiabatic instability) is given by

$$\Theta > 1 \tag{11}$$

with

$$\Theta \equiv \frac{H^* \sigma \varepsilon}{nhRT^2 \rho C_P} \beta \tag{12}$$

where H^* is the activation enthalpy for deformation, n the stress exponent (Eq. (5)), h a parameter that is related to the hardening effect ($h \sim 0.1$), ε strain, ρ density, C_P specific heat and β a parameter that measures the efficiency of conversion of mechanical energy to heat defined by

$$\beta = 1 - \exp\left(-\frac{\dot{\varepsilon} L^2}{\kappa}\right) \tag{13}$$

where L is the size of the region and κ thermal diffusivity. A similar equation can be derived for a highly non-linear mechanism such as the Peierls mechanism (Kameyama et al., 1999). Eqs. (11)–(13) mean that both low temperature and a high strain-rate are needed for thermal runaway instability. Such a condition is
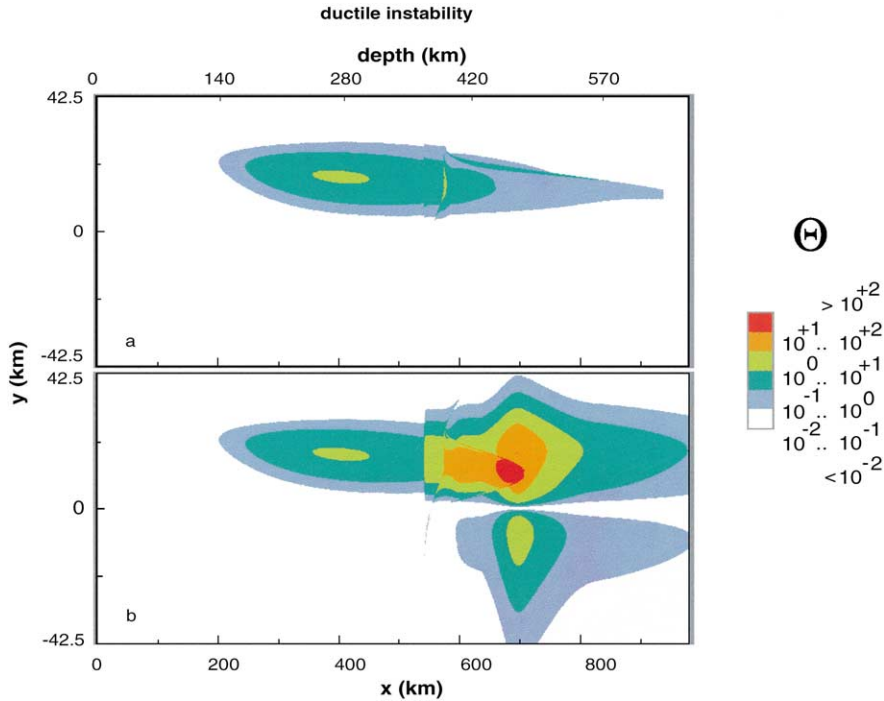
Fig. 8. Distribution of the instability parameter Θ in subducted slabs with $v_{sub} = 10$ cm per year (a) for a case where the effects of latent heat release and grain-size reduction are neglected (corresponding to a broken curve in Fig. 6) and (b) for a case where the effects of latent heat release and grain-size reduction are included. When this parameter exceeds ~ 1, thermal runaway instability occurs. For a cold slab (10 cm per year), Θ in high strength regions surrounding a weak, fine-grained spinel core in the deep slab exceeds the critical value for thermal runaway instability. Deep earthquakes likely nucleate in these regions. In this case one expects a double seismic zone as seen by Wiens et al. (1993). The width of the seismogenic regions is estimated to be ~ 40–60 km. Note also that the instability criterion is also satisfied in the shallow portions, providing explanation for intermediate earthquakes.

not usually met because high strain-rates are usually associated with high temperatures. However, because of the overall weakening of slabs (low flexural rigidity) at low temperature conditions, these conditions are likely to be met in deep slabs. The validity of instability criterion (11) is largely confirmed by finite amplitude calculations such as by Kameyama et al. (1999).

Fig. 8 shows plots of Θ. When this parameter becomes larger than ~ 1, thermal runaway instability will occur. Three points must be noted. First, in the deep cold slab, regions surrounding the weak, fine-grained spinel core likely satisfy this instability criterion. Second, the instability conditions are met also at the shallower depths and can therefore explain the occurrence of intermediate depth earthquakes. Third, the effects of grain-size reduction and the latent heat release associated with the olivine–spinel phase transformation

significantly enhances deep earthquake activity (compare Fig. 8a and b).

The model of thermal runaway for deep earthquakes combined with our slab rheology model has some interesting features. First, our model provides a natural explanation for large dimensions of faults observed to be associated with deep earthquakes. In this model, earthquake faulting likely occurs in high strength regions when the strain-rate is high. In cold slabs, these would be the regions surrounding a weak, fine-grained spinel core (Fig. 8b). Thus, our model provides a natural explanation for the observed double seismic zones of deep earthquakes (Wiens et al., 1993) and gives a robust estimate of the width of the seismogenic region to be 40–60 km. This predicted fault width is in excellent agreement with seismological observations of the width of deep earthquake fault zones (Kikuchi

and Kanamori, 1994; Wiens et al., 1994). It should be noted that the width of the fault zone for the 1994 Fiji earthquake is determined from the observations of aftershocks. Therefore the faults must have *nucleated* in a wide seismogenic zone rather than propagating to the observed dimensions. Note that thermal instability could also occur in relatively warm slabs if a large enough moment is applied (not shown here). In this case, the presence of a metastable olivine wedge is not required for deep earthquakes. The seismogenic regions would correspond to high strength regions in relatively cold portions of slabs. The width of the seismogenic zone depends on the magnitude of the bending moment and is estimated to be 30–60 km. In contrast to our model, the transformation faulting model proposed previously (Kirby, 1987; Green and Burnley, 1989; Kirby et al., 1991) clearly fails to account for this important observation and is therefore no longer a tenable model for deep earthquakes. In addition, a different mechanism is needed to explain intermediate earthquakes in the transformation faulting mode, which also makes this model less attractive.

How does this thermal instability model explain some of the other characteristics of deep earthquakes? The depth variation of seismicity is characterized by a continuous decrease down to ∼400 km followed by a peak in seismicity at around 550–600 km and finally there is a sharp cutoff at ∼680 km (e.g. Frohlich, 1989). The present model provides a clear explanation for the peak at around 550–600 km. Our model predicts that the strain-rates should be high in this depth region because of the low flexural rigidity. A high stress concentration in high strength regions surrounding a weak, fine-grained spinel core enhances the thermal runaway instability in this depth region. A large magnitude of latent heat release in the deep portions of slabs will also enhance thermal runaway instabilities (Bina, 1998). Intermediate depth earthquakes that occur from ∼200 to ∼400 km depth region may also be attributed to thermal runaway instability, because warm regions of slabs in this depth region could satisfy the necessary condition for thermal runaway instability (Hobbs and Ord, 1988; Fig. 8). A clear shutoff of seismicity at a depth of ∼680 km is most likely due to the loss of strength of slabs in the lower mantle due to superplasticity (Ito and Sato, 1990; Karato et al., 1995) and/or to the absence of strong forces in this depth region.

Kanamori et al. (1998), Estabrook (1999) and Wiens (this volume) showed that deep earthquakes are characterized by low seismic efficiency and slow rupture velocity, particularly those that occur in warm slabs. Kanamori et al. (1998) argued that a thermal instability model provides a natural explanation for the low seismic efficiency: thermal runaway instability involves significant plastic flow and therefore some of the stored energy is dissipated as heat.

Another characteristic of deep earthquakes is the low frequency of aftershocks, particularly those with small magnitude (e.g. Frohlich, 1989). Wiens and Gilbert (1996) (see Wiens, this volume) also showed that the aftershock frequency tends to be lower for warmer slabs particularly for those with small magnitudes (which leads to lower *b* values in the Gutenberg–Richter relation for warm slabs). Other correlations between fault characteristics and slab temperature include those seismic efficiency and the nature of the source–time function (Estabrook, 1999). The thermal runaway instability model provides a natural explanation for these observations. Thermal runaway instability is scale-dependent because it is sensitive to the time scale of deformation relative to the time scale of thermal diffusion which depends on the length scale of deformation (see Eq. (13)). Consequently, small scale instabilities that would result in earthquakes with small magnitudes are difficult to realize through this process (for the same reason, laboratory studies of adiabatic instability is difficult; one needs an exceedingly high strain-rate to produce an adiabatic instability in a small sample; Kitamura et al., 1992).

5. Concluding remarks

In most laboratory experiments or numerical modeling of convection or slab deformation, a simple rheology for Earth materials, such as constant viscosity or a very weakly temperature dependent viscosity, has been assumed. This is firstly due to computational difficulties in incorporating more "realistic" rheologies but also because if one uses such "realistic" rheologies (strongly temperature-dependent rheology), one would not see much deformation of slabs (Davies, 1995). These studies have led to the notion that it is mainly the kinematic boundary conditions that control

the variation in deformation behavior of slabs and the importance of the rheology of slabs has not been well appreciated. We have shown from both theoretical and observational backgrounds that realistic slab rheology must be considered as an important parameter that plays a critical role in slab deformation when the nature of slab-transition zone interaction is investigated. Consideration of realistic rheology is also critical in understanding the mechanisms of deep earthquakes.

The key features of our model are a strong dependence of the grain-size of spinel on temperature and a highly stress-dependent rheology through power-law creep and the Peierls mechanism. We used a theoretical model to estimate grain-size and experimental data on deformation of olivine and spinel (ringwoodite). Although many of the rheological parameters for high pressure minerals are poorly constrained, these qualitative features are well documented in material science (e.g. Frost and Ashby, 1982) and seem robust. In fact, recent direct high-pressure deformation experiments of silicate spinel (ringwoodite) demonstrate the important role of grain-size sensitive creep at small grain-sizes (Karato et al., 1998).

We have focused on slab deformation above the 660 km discontinuity. This is firstly because the deformability of slabs in that region controls their fate upon collision with the 660 km discontinuity, and secondly because much less is known about the rheology and the kinetics of phase transformations for lower mantle minerals. However, most results of seismic tomography show significant thickening of slabs in the lower mantle (van der Hilst et al., 1997; Bijwaard et al., 1998), suggesting that slabs there are weak. Effects of grain-size reduction, as investigated in this study, may also operate in the lower mantle (Ito and Sato, 1990; Kubo et al., 2000).

Finally, if some slabs are indeed weak in the deep transition zone, as our model suggests, then the role of the 660 km discontinuity to modify convection patterns must be significant. Such an effect would be more pronounced at high Rayleigh numbers (Christensen and Yuen, 1985), therefore the convection style could have evolved with time as mantle temperatures and hence Rayleigh number has changed (Breuer and Spohn, 1995; Honda, 1995). Thus, the nature of interaction of convection currents with the 660 km discontinuity is likely to vary both regionally and temporally. Rheology of mantle materials, particularly that

of subducting slabs, appears to play an important role in controlling the complexity of mantle convection.

References

Akaogi, M., Ito, E., Navrotsky, A., 1989. Olivine-modified spinel–spinel transitions in the system Mg_2SiO_4–Fe_2SiO_4: calorimetric measurements, thermochemical calculation, and geophysical application. J. Geophys. Res. 94, 15671–15685.

Axe, J.D., Yamada, Y., 1986. Scaling relations for grain autocorrelation functions during nucleation and growth. Phys. Rev. B89, 10161–10177.

Backofen, W.A., 1972. Deformation Processing. Addison-Wesley, Reading, MA.

Basinski, Z.S., 1957. The instability of plastic deformation of metals at very low temperatures. Proc. R. Soc. London Ser. A 240, 229–242.

Basinski, Z.S., 1960. The instability of plastic deformation of metals at very low temperatures, II. Aust. J. Phys. 13, 354–358.

Bijwaard, H., Spakman, W., Engdahl, E.R., 1998. Closing the gap between regional and global travel time tomography. J. Geophys. Res. 103, 30055–30078.

Bina, C.R., 1996. Phase transition buoyancy contributions to stresses in subducting lithosphere. Geophys. Res. Lett. 23, 3563–3566.

Bina, C.R., 1997. Patterns of deep seismicity reflect buoyancy stresses due to phase transitions. Geophys. Res. Lett. 24, 3301–3304.

Bina, C.R., 1998. A note on latent heat release from disequilibrium phase transformations and deep seismogenesis. Earth Planet. Space 50, 1029–1034.

Branlund, J.M., Kameyama, M., Yuen, D.A., Kaneda, Y., 2000. Effects of temperature-dependent thermal diffusivity on shear instability in a viscoelastic zone: implications for faster ductile faulting and earthquakes in the spinel stability field. Earth Planet. Sci. Lett. 182, 171–185.

Breuer, D., Spohn, T., 1995. Possible flush instability in mantle convection at the Archean-Proterozoic transition. Nature 378, 608–610.

Castle, J.C., Creager, K.C., 1998. Topography of the 660 km seismic discontinuity beneath Izu–Bonin: implications for the tectonic history and slab deformation. J. Geophys. Res. 103, 12511–12527.

Chapple, W.M., Tullis, T.E., 1977. Evaluation of the forces that drive the plates. J. Geophys. Res. 82, 1967–1984.

Chen, J., Inoue, T., Weidner, D.J., Wu, Y., Vaughan, M.T., 1998. Strength and water weakening of mantle minerals, olivine, wadsleyite and ringwoodite. Geophys. Res. Lett. 25, 575–578.

Christensen, U.R., 1996. The influence of trench migration on slab penetration into the lower mantle. Earth Planet. Sci. Lett. 140, 27–39.

Christensen, U.R., Yuen, D.A., 1984. The interaction of a subducting lithospheric slab with a chemical or phase-boundary. J. Geophys. Res. 89, 4389–4402.

Christensen, U.R., Yuen, D.A., 1985. Layered convection induced by phase-transitions. J. Geophys. Res. 90, 291–300.

Daessler, R., Yuen, D.A., Karato, S., Riedel, M.R., 1996. Two-dimensional thermo-kinetic model for the olivine–spinel transition in subducting slabs. Phys. Earth Planet. Inter. 94, 217–239.

Davies, G.F., 1980. Mechanics of subducted lithosphere. J. Geophys. Res. 85, 6304–6318.

Davies, G.F., 1995. Penetration of plates and plumes through the mantle transition zone. Earth Planet. Sci. Lett. 133, 507–516.

Ding, X.-Y., Grand, S.P., 1994. Seismic structure of the deep Kurile subduction zone. J. Geophys. Res. 99, 23767–23786.

Dupas-Bruzek, C., Sharp, T.G., Rubie, D.C., Durham, W.B., 1998. Mechanisms of transformation and deformation in $Mg_{1.8}Fe_{0.2}SiO_4$ olivine and wadsleyite under non-hydrostatic stress. Phys. Earth Planet. Inter. 108, 33–48.

Engdahl, E.R., van der Hilst, R.D., Berrocal, J., 1995. Imaging of subducted lithosphere beneath South America. Geophys. Res. Lett. 22, 2317–2320.

Engdahl, E.R., van der Hilst, R.D., Buland, R.P., 1998. Global teleseismic earthquake relocation with improved travel times and procedures for depth determination. Bull. Seism. Soc. Am. 88, 722–743.

Estabrook, C.H., 1999. Body wave inversion of the 1970 and 1963 South American large deep-focus earthquakes. J. Geophys. Res. 104, 28751–28767.

Estrin, Y., Kubin, L.P., 1988. Plastic instabilities: classification and physical mechanisms. Res. Mechanics 23, 197–221.

Evans, B., Goetze, C., 1979. Temperature variation of hardness of olivine and its implication for polycrystalline yield stress. J. Geophys. Res. 84, 5505–5524.

Forsyth, D.W., Uyeda, S., 1975. On the relative importance of driving forces of plate motion. Geophys. J. R. Astr. Soc. 43, 163–200.

Fressengeas, C., Molinari, A., 1987. Instability and localization of plastic flow in shear at high strain rate. J. Mech. Phys. Solids 35, 185–211.

Frohlich, C., 1989. The nature of deep focus earthquakes. Ann. Rev. Earth Planet. Sci. 17, 227–254.

Frost, H.J., Ashby, M.F., 1982. Deformation Mechanism Maps. Pergamon Press, Oxford, p. 168.

Fukao, Y., Obayashi, M., Inoue, H., Nenbai, M., 1992. Subducting slabs stagnant in the mantle transition zone. J. Geophys. Res. 97, 4809–4822.

Giardini, D., 1992. Space-time distribution of deep seismic deformation in Tonga. Phys. Earth Planet. Inter. 74, 75–88.

Giardini, D., Woodhouse, J.H., 1984. Deep seismicity and modes of deformation in Tonga subduction zone. Nature 307, 505–509.

Gordon, R.B., 1971. Observations of crystal plasticity under pressure with application to the Earth's mantle. J. Geophys. Res. 76, 2413–2418.

Grand, S., 1994. Mantle shear structure beneath the Americas and surrounding oceans. J. Geophys. Res. 99, 11591–11621.

Green II, H.W., 1994. Solving the paradox of deep earthquakes. Sci. Am. 271, 64–71.

Green II, H.W., Burnley, P.C., 1989. A new self-organizing mechanism for deep focus earthquakes. Nature 341, 733–737.

Green II, H.W., Houston, H., 1995. The mechanics of deep earthquakes. Ann. Rev. Earth Planet. Sci. 23, 169–213.

Green II, H.W., Zhou, Y., 1996. Transformation-induced faulting requires an endothermic reaction and explains the cessation of earthquakes at the base of the mantle transition zone. Tectonophysics 256, 39–56.

Green II, H.W., Young, T.E., Walker, D., Scholtz, C., 1990. Anticrack-associated faulting at very high pressure in natural olivine. Nature 348, 720–722.

Greenwood, G.W., Johnson, R.H., 1965. Deformation of metals at small stresses during phase transformations. Proc. Roy. Soc. Ser A 283, 403–422.

Griffths, R.W., Hackney, R.I., van der Hilst, R.D., 1996. A laboratory investigation of effects of trench migration on the descent of subducted slabs. Earth Planet. Sci. Lett. 133, 1–17.

Griggs, D.T., Baker, D.W., 1969. The origin of deep focus earthquakes. In: Mark, H., Fernbach, S. (Eds.), Properties of Matter Under Unusual Conditions. Wiley/Intersciences, New York, pp. 23–42.

Guillou-Frottier, L., Buttles, J., Olson, P., 1996. Laboratory experiments on the structure of subducted lithosphere. Earth Planet. Sci. Lett. 133, 19–34.

Gurnis, M., Hager, B.H., 1988. Controls of the structure of subducted slabs. Nature 335, 317–321.

Hager, B.H., O'Connell, R.J., 1978. Subduction zone dip and flow driven by plate motions. Tectonophysics 50, 111–133.

Hirth, G., Kohlstedt, D.L., 1995a. Experimental constraints on the dynamics of the partially molten upper mantle: deformation in the diffusion creep regime. J. Geophys. Res. 100, 1981–2001.

Hirth, G., Kohlstedt, D.L., 1995b. Experimental constraints on the dynamics of the partially molten upper mantle. 2. Deformation in the dislocation creep regime. J. Geophys. Res. 100, 15441–15450.

Hirth, G., Kohlstedt, D.L., 1996. Water in the oceanic upper mantle: implications for rheology, melt extraction and the evolution of the lithosphere. Earth Planet. Sci. Lett. 144, 93–108.

Hobbs, B.E., Ord, A., 1988. Plastic instabilities: implications for the origin of intermediate and deep focus earthquakes. J. Geophys. Res. 93, 10521–10540.

Holt, W.E., 1995. Flow fields within the Tonga slab determined from the moment tensors of deep earthquakes. Geophys. Res. Lett. 22, 989–992.

Honda, S., 1995. A simple parameterized model of Earth's thermal history with the transition from layered to whole mantle convection. Earth Planet. Sci. Lett. 131, 357–370.

Honda, S., Yuen, D.A., Balachandar, S., Reuteler, D., 1993. Three-dimensional mantle dynamics with an endothermic phase transition. Science 259, 1308–1311.

Houseman, G.A., Gubbins, D., 1997. Deformation of subducted oceanic lithosphere. Geophys. J. Int. 131, 535–551.

Irifune, T., Kuroda, K., Funamori, N., Uchida, T., Yagi, T., Inoue, T., Miyajima, N., 1996. Amorphization of serpentine at high pressure and high temperature. Science 272, 1468–1470.

Isacks, B.L., Molner, P., 1969. Mantle earthquakes mechanisms and the sinking of the lithosphere. Nature 223, 1121–1124.

Isacks, B.L., Barazangi, M., 1977. Geometry of Benioff zones: lateral segmentation and downward bending of the subducted lithosphere. In: Talwani, M., Pitman III, W.C. (Eds.), Island Arcs, Deep Sea Trenches and Back-Arc Basins. American Geophysics Union, Washington, DC, pp. 99–114.

Ito, E., Sato, H., 1990. Aseismicity in the lower mantle by superplasticity in a subducting slab. Nature 351, 140–141.

Jarrard, R.D., 1986. Relations among subduction parameters. Rev. Geophys. 24, 217–284.

Kameyama, M., Yuen, D.A., Karato, S., 1999. Thermal–mechanical effects of low-temperature plasticity (the Peierls mechanism) on the deformation of a viscoelastic shear zone. Earth Planet. Sci. Lett. 168, 159–172.

Kanamori, H., Anderson, D.L., 1975. Theoretical basis of some empirical relations in seismology. Bull. Seism. Soc. Am. 65, 1073–1095.

Kanamori, H., Anderson, D.L., Heaton, T.H., 1998. Frictional melting during the rupture of the 1994 Bolivia earthquake. Science 279, 839–842.

Karato, S., 1986. Does partial melting reduce the creep strength of the upper mantle. Nature 319, 309–310.

Karato, S., 1989a. Plasticity-crystal structure systematics in dense oxides and its implications for the creep strength of the Earth's deep interior: a preliminary result. Phys. Earth Planet. Inter. 55, 234–240.

Karato, S., 1989b. Grain growth kinetics in olivine aggregates. Tectonophysics 155, 255–273.

Karato, S., 1997a. On the separation of crustal component from subducted oceanic lithosphere near the 660 km discontinuity. Phys. Earth Planet. Inter. 99, 103–111.

Karato, S., 1997b. Phase transformations and rheological properties of mantle minerals. In: Crossley, D. (Ed.), Earth's Deep Interior (Doornbus Volume). Gordon and Breach, pp. 223–272.

Karato, S., 1998. Effects of pressure on plastic deformation of polycrystalline solids: some geological applications. In: Wentzcovitch, R.M., Hemley, R.J., Nellis, W.J., Yu, P.Y. (Eds.), High Pressure Research in Materials Research. Materials Research Society, Warrendale, PA, pp. 3–14.

Karato, S., Rubie, D.C., 1997. Toward an experimental study of deep mantle rheology: a new multianvil sample assembly for deformation studies under high pressure and temperatures. J. Geophys. Res. 102, 20111–20122.

Karato, S., Jung, H., 1998. Water, partial melting and the origin of the seismic low velocity and high attenuation zone in the upper mantle. Earth Planet. Sci. Lett. 157, 193–207.

Karato, S., Wu, P., 1993. Rheology of the upper mantle: A synthesis. Science 260, 771–778.

Karato, S., Paterson, M.S., Fitz Gerald, J.D., 1986. Rheology of synthetic olivine aggregates: influence of grain size and water. J. Geophys. Res. 91, 8151–8176.

Karato, S., Rubie, D.C., Yan, H., O'Neill, St.H.C., 1993. Dislocation recovery in olivine under deep upper mantle conditions. J. Geophys. Res. 98, 9761–9768.

Karato, S., Zhang, S., Wenk, H.-R., 1995. Superplasticity in Earth's lower mantle: evidence from seismic anisotropy and rock physics. Science 270, 458–461.

Karato, S., Dupas-Bruzek, C., Rubie, D.C., 1998. Plastic deformation of silicate spinel under the transition zone conditions of the Earth. Nature 395, 266–269.

Kerschhofer, L., Sharp, T.G., Rubie, D.C., 1996. Intracrystalline transformation of olivine to wadsleyite and ringwoodite under subduction zone conditions. Science 274, 79–81.

Kerschhofer, L., Dupas, C., Liu, M., Sharp, T.G., Durham, W.B., Rubie, D.C., 1998. Polymorphic transformations between olivine, wadsleyite and ringwoodite: mechanisms of intracrystalline transformation and role of elastic strain. Mineral. Mag. 62, 617–638.

Kerschhofer, L., Rubie, D.C., Sharp, T.G., McConnell, J.D.C., Dupas-Bruzek, C., 2000. Kinetics of intracrystalline olivine–ringwoodite transformation. Phys. Earth Planet. Inter. 121, 59–76.

Kikuchi, M., Kanamori, H., 1994. The mechanism of the deep Bolivia earthquake of June 9, 1994. Geophys. Res. Lett. 22, 2341–2344.

Kincaid, C., Olson, P., 1987. An experimental study of subduction and slab migration. J. Geophys. Res. 92, 13832–13840.

King, S.D., Ita, J.J., 1995. Effect of slab rheology on mass transport across a phase transition boundary. J. Geophys. Res. 100, 20211–20222.

Kirby, S.H., 1987. Localized polymorphic phase transformations in high-pressure faults and applications to the physical mechanisms of deep earthquakes. J. Geophys. Res. 92, 13789–13800.

Kirby, S.H., Durham, W.B., Stern, L., 1991. Mantle phase changes and deep-earthquake faulting in subducting slabs. Science 252, 216–225.

Kirby, S.H., Stein, S., Okal, E.A., Rubie, D.C., 1996. Metastable mantle phase transformations and deep earthquakes in subducting oceanic lithosphere. Rev. Geophys. 34, 261–306.

Kitamura, M., Tsuchiyama, A., Watanabe, S., Syono, Y., Fukuoka, K., 1992. Shock recovery experiments on chondritic materials. In: Syono, Y., Manghnani, M.H. (Eds.), High-Pressure Research: Application to Earth and Planetary Sciences. Terra Science Publication, Tokyo, pp. 333–340.

Kubo, T., Ohtani, E., Kato, T., Shinmei, T., Fujino, K., 1998a. Effects of water on the α–β transformation kinetics in San Carlos olivine. Science 281, 85–87.

Kubo, T., Ohtani, E., Kato, T., Shinmei, T., Fujino, K., 1998b. Experimental investigation of the α–β transformation of San Carlos olivine single crystals. Phys. Chem. Mineral. 26, 1–6.

Kubo, T., Ohtani, E., Kato, T., Urakawa, S., Suzuki, A., Kanbe, Y., Funakoshi, K., Utsumi, W., Fujino, K., 2000.

Formation of metastable assemblages and mechanisms of the grain-size reduction in the postspinel transformation of Mg_2SiO_4. Geophys. Res. Lett. 27, 807–810.

Lawlis, J.D., Lee, K.-H., Frost, D., Rubie, D.C., Cordier, P., Karato, S., 1999. Deformation and fabric development in transition zone minerals. EOS 80, F975.

Lawlis, J.D., Zhang, Y., Karato, S., 2001. High-temperature creep in Ni_2GeO_4: A contribution to creep systematics in spinel. Chem. Mineral., in press.

Lithgow-Bertelloni, C., Richards, M.A., 1998. The dynamics of Cenozoic and Mesozoic plate motions. Rev. Geophys. 36, 27–78.

Liu, M., 1997. A constitutive model for olivine–spinel aggregates and its application to deep earthquake nucleation. J. Geophys. Res. 102, 5295–5312.

Lundgren, P.R., Giardini, D., 1992. Seismicity, shear failure and modes of deformation in deep subduction zones. Phys. Earth Planet. Inter. 74, 63–74.

Marton, F., Bina, C.R., Stein, S., Rubie, D.C., 1999. Effects of slab mineralogy on subduction rates. Geophys. Res. Lett. 26, 119–122.

McKenzie, D.P., 1969. Speculations on the consequences and causes of plate motions. Geophys. J. R. Astr. Soc. 18, 1–32.

Meade, C., Jeanloz, R., 1991. Deep-focus earthquakes and recycling of water into the Earth's mantle. Science 252, 68–72.

Meike, A., 1993. A critical review of investigations into transformational plasticity. In: Boland, J.N., Fitz Gerald, J.D. (Eds.), Defects and Processes in the Solid States: Geoscience Applications. Elsevier, Amsterdam, pp. 5–25.

Moresi, L., Gurnis, M., 1996. Constraints on the lateral strength of slabs from three-dimensional dynamic flow models. Earth Planet. Sci. Lett. 138, 15–28.

Mosenfelder, J.L., Connelly, J.A.D., Rubie, D.C., Liu, M., 2000. Strength of $(Mg, Fe)_2SiO_4$ wadsleyite determined by relaxation of transformational stress. Phys. Earth Planet. Inter. 120, 63–78.

Obata, M., Karato, S., 1995. Ultramafic pseudotachylyte from Balmuccia peridotite, Ivrea–Verbana zone, northern Italy. Tectonophysics 242, 313–328.

Ogawa, M., 1987. Shear instability in a viscoelastic material as the cause for deep focus earthquakes. J. Geophys. Res. 92, 13801–13810.

Ohtani, E., 1983. Melting temperature distribution and fractionation in the lower mantle. Phys. Earth Planet. Inter. 33, 12–25.

Okamoto, Y., 1989. Creep deformation mechanisms in oxides and deformation of spinel ferrites. In: Karato, S., Toriumi, M. (Eds.), Rheology of Solids and of the Earth. Oxford University Press, Oxford, pp. 83–104.

Olbertz, D., 1997. The long-term evolution of subduction zones: a modelling study. Ph.D. thesis, University of Utrecht, p. 152.

Olbertz, D., Wortel, M.J.R., Hansen, U., 1997. Trench migration and subduction zone geometry. Geophys. Res. Lett. 24, 221–224.

O'Neill, B., Jeanloz, R., 1994. $MgSiO_3$–$FeSiO_3$–Al_2O_3 in the Earth's lower mantle: perovskite and garnet at 1200 km depth. J. Geophys. Res. 99, 19901–19915.

Panasyuk, S.V., Hager, B.H., 1998. A model of transformational superplasticity in the upper mantle. Geophys. J. Int. 133, 741–755.

Paterson, M.S., 1983. Creep in transforming polycrystalline materials. Mech. Mater. 2, 103–109.

Poirier, J.-P., 1980. Shear localization and shear instability in materials in the ductile field. J. Struct. Geol. 2, 135–142.

Poirier, J.-P., 1982. On transformation plasticity. J. Geophys. Res. 87, 6791–6797.

Presnall, D.C., Walker, M.J., 1993. Melting of forsterite, Mg_2SiO_4, from 9.7 to 16.5 GPa. J. Geophys. Res. 98, 19777–19783.

Riedel, M.R., Karato, S., 1996. Microstructural development during nucleation and growth. Geophys. J. Int. 125, 397–414.

Riedel, M.R., Karato, S., 1997. Grain-size evolution in subducted oceanic lithosphere associated with the olivine–spinel transformation and its influence on rheology. Earth Planet. Sci. Lett. 148, 27–44.

Riedel, M.R., Karato, S., Yuen, D.A., 1998. Criticality of subducting Slabs. EOS, 79, F911.

Ringwood, A.E., 1991. Phase transformations and their bearings on the constitution and dynamics of the mantle. Geochim. Cosmochim. Acta 55, 2083–2110.

Ringwood, A.E., Irifune, T., 1988. Nature of the 650 km seismic discontinuity. Nature 331, 131–136.

Rogers, H.C., 1979. Adiabatic plastic deformation. Ann. Rev. Mater. Sci. 9, 283–311.

Rubie, D.C., 1984. The olivine–spinel transformation and the rheology of subducting lithosphere. Nature 308, 505–508.

Rubie, D.C., Ross II, C.R., 1994. Kinetics of the olivine–spinel transformation in subducting lithosphere: experimental constraints and implications for deep slab processes. Phys. Earth Planet. Inter. 86, 223–241.

Rubie, D.C., Tsuchida, Y., Yagi, T., Utsumi, W., Kikegawa, T., Shimomura, O., Brearley, A.J., 1990. An in situ X-ray diffraction study of the kinetics of the Ni_2SiO_4 olivine–spinel transformation. J. Geophys. Res. 95, 15829–15844.

Rubie, D.C., Mosenfelder, J.L., Kerschhofer, L., 1998. Mechanisms of grain size reduction and rheological weakening in subducting slabs. EOS 79, F911.

Sakurai, T., 1996. Whole mantle P-wave tomography and differential PP–P time measurement. M.Sc. thesis, University of Tokyo, p. 31.

Sammis, C.G., Dein, J.L., 1974. On the possibility of transformational superplasticity in the Earth's mantle. J. Geophys. Res. 79, 2961–2965.

Schmeling, H., Monz, R., Rubie, D.C., 1999. The influence of olivine metastability on the dynamics of subduction. Earth Planet. Sci. Lett. 165, 55–66.

Shimizu, I., 1998. Stress and temperature dependence of recrystallized grain size: a subgrain misorientation model. Geophys. Res. Lett. 25, 4237–4240.

Silver, P.G., Beck, S.L., Wallace, T.C., Meade, C., Myers, S.C., James, D.E., Kuehnel, R., 1995. Rupture characteristics of the deep Bolivia earthquakes of 9 June 1994 and the mechanism of deep-focus earthquakes. Science 268, 69–71.

Staker, M.R., 1981. The relation between adiabatic shear instability, strain and material properties. Acta Metall. 29, 683–689.

Sugi, N., Kikuchi, M., Fukao, Y., 1989. Mode of stress release within a subducting slab of lithosphere: implications of source mechanism of deep and intermediate-depth earthquakes. Phys. Earth Planet. Inter. 55, 106–125.

Tackley, P.J., 1997. Effects of phase transitions on three-dimensional mantle convection. In: Crossley, D.J. (Ed.), Earth's Deep Interior. Gordon and Breach Science Publisher, Amsterdam, pp. 273–335.

Tackley, P.J., Stevenson, D.J., Glatzmaier, G.A., Schubert, G., 1993. Effects of an endothermic phase-transition at 670 km depth in a spherical model of convection in the Earth's mantle. Nature 361, 699–704.

Tibi, R., Estabrook, C.H., Bock, G., 1999. The 1996 June 17 Flores Sea and 1994 March 9 Fiji-Tonga earthquakes: source processes and deep earthquake mechanisms. Geophys. J. Int. 128, 625–642.

Tingle, T.N., Green II, H.W., Scholtz, C.H., Koczynski, T.A., 1993. The rheology of faults triggered by the olivine–spinel transformation in Mg_2GeO_4 and its implications for the mechanism of deep focus earthquakes. J. Struct. Geol. 15, 1249–1256.

Turcotte, D.L., Schubert, G., 1982. Geodynamics. Wiley, New York.

van der Hilst, R.D., 1995. Complex morphology of subducted lithosphere in the mantle beneath the Tonga trench. Nature 374, 154–157.

van der Hilst, R.D., Seno, T., 1993. Effects of relative plate motion on the deep structure and penetration depth of slabs below the Izu–Bonin and Mariana arcs. Earth Planet. Sci. Lett. 120, 395–407.

van der Hilst, R.D., Engdahl, E.R., Spakman, W., Nolet, G., 1991. Tomographic imaging of subducted lithosphere below northwest Pacific island arcs. Nature 353, 37–43.

van der Hilst, R.D., Widiyantoro, S., Engdahl, E.R., 1997. Evidence for deep mantle circulation from global tomography. Nature 386, 578–584.

Vaughan, P.J., Coe, R.S., 1981. Creep mechanisms in Mg_2GeO_4: effects of a phase transition. J. Geophys. Res. 86, 389–404.

Vogt, P.R., Lowrie, A., Bracey, D.R., Hey, R.N., 1976. Subduction of aseismic oceanic ridges: effects on shape, seismicity and other characteristics of consuming plate boundaries. Special Paper 162. Geological Society of America, p. 59.

Weertman, J., 1968. Dislocation climb theory of steady-state creep. Trans. ASM 61, 681–694.

Wiens, D.A., Gilbert, H.J., 1996. Effect of slab temperature on deep-earthquake aftershock productivity and magnitude–frequency relations. Nature 372, 153–156.

Wiens, D.A., Snider, N.O., 1999. Repeating deep earthquakes: evidence for fault reactivation at great depth. EOS, Trans. Am. Geophys. Union 80, F667.

Wiens, D.A., McGuire, J.J., Shore, P.J., 1993. Evidence for transformational faulting from a deep double seismic zone in Tonga. Nature 364, 790–793.

Wiens, D.A., McGuire, J.J., Shore, P.J., Bevis, M.G., Draunidalo, K., Prasad, G., Helu, S.P., 1994. A deep earthquake aftershock sequence and implications for the rupture mechanism of deep earthquakes. Nature 372, 540–543.

Wortel, M.J.R., Vlaar, N.J., 1988. Subduction zone seismicity and the thermo-mechanical evolution of down-going lithosphere. PAGEOPH 128, 625–659.

Yamaoka, K., Fukao, Y., Kumazawa, M., 1986. Spherical shell tectonics: effect of sphericity and inextensibility on the geometry of the descending lithosphere. Rev. Geophys. 24, 27–53.

Yoshioka, S., Daessler, D., Yuen, D.A., 1997. Stress fields associated with metastable phase transitions in descending slabs and deep-focus earthquakes. Phys. Earth Planet. Inter. 104, 345–361.

Zhao, Y.-H., Lawlis, J.D., Lee, K.-H., Karato, S., 1999. Deformation of $(Mg, Ni)_2GeO_4$: the effects of the olivine–spinel transformation. EOS 80, 1027–1028.

Zhong, S.J., Gurnis, M., 1995. Mantle convection with plates and mobile, faulted plate margins. Science 267, 838–843.

Zhong, S., Davies, G.F., 1999. Effects of plate and slab viscosities on the geoid. Earth Planet. Sci. Lett. 170, 487–496.